The HKU Scholars Hub The University of Hong Kong 香港大學學術庫

Title	Effects of corticosterone and amyloid-beta on proteins essential for synaptic function: Implications for depression and Alzheimer's disease.
Author(s)	WUWONGSE, S; CHENG, SY; WONG, THG; HUNG, HL; ZHANG, Q; HO, YS; Law, ACK; Chang, RCC
Citation	Biochimica et Biophysica Acta: Molecular Basis of Disease, 2013, v. 1832 n. 12, p. 2245-2256
Issued Date	2013
URL	http://hdl.handle.net/10722/188857
Rights	NOTICE: this is the author's version of a work that was accepted for publication in Biochimica et Biophysica Acta: Molecular Basis of Disease. Changes resulting from the publishing process, such as peer review, editing, corrections, structural formatting, and other quality control mechanisms may not be reflected in this document. Changes may have been made to this work since it was submitted for publication. A definitive version was subsequently published in Biochimica et Biophysica Acta: Molecular Basis of Disease, 2013, v. 1832 n. 12, p. 2245-2256. DOI: 10.1016/j.bbadis.2013.07.022

*REVISED Manuscript (text UNmarked)
Click here to view linked References

Effects of corticosterone and amyloid-beta on proteins essential for synaptic function: Implications for depression and Alzheimer's disease

Suthicha WUWONGSE[1,2], Sally Shuk-Yee CHENG[2], Ginger Tsz-Hin WONG[1,2], Clara Hiu-Ling HUNG[2], Natalie Qishan ZHANG[2], , Yuen-Shan HO[2,5], Andrew Chi-Kin LAW[1,3,4], Raymond Chuen-Chung CHANG[2,3,4]

[1]Neurodysfunction Research Laboratory, Department of Psychiatry,

[2]Laboratory of Neurodegenerative Diseases, Department of Anatomy,

[3]Research Centre of Heart, Brain, Hormone and Healthy Aging,

LKS Faculty of Medicine

[4]State Key Laboratory of Brain and Cognitive Sciences, The University of Hong Kong, Pokfulam, Hong Kong SAR, CHINA

[5]State Key Laboratory of Quality Research in Chinese Medicine, Macau University of Science and Technology, Macau SAR, CHINA

Running Title: Effects of corticosterone and amyloid-beta on synaptic proteins

Address for correspondence:

Dr. Raymond Chuen-Chung CHANG

Department of Anatomy, LKS Faculty of Medicine, & State Key Laboratory of Brain and Cognitive Sciences, The University of Hong Kong, Rm. L1-49, Laboratory Block, Faculty of Medicine Building, 21 Sassoon Road, Pokfulam, Hong Kong SAR

Fax: (+852) 2817-0857; E-mail: rccchang@hku.hk

or

Dr. Andrew CK LAW,

Department of Psychiatry, The University of Hong Kong, Room 219, Block J, Queen Mary Hospital, 102 Pokfulam Road, Pokfulam, Hong Kong SAR

Fax: (+852) 2819-3851; E-mail: acklaw@hku.hk

Abstract

The relationship between Alzheimer's disease (AD) and depression has been well established in terms of epidemiological and clinical observations. Depression has been considered to be both a symptom and risk factor of AD. Several genetic and neurobiological mechanisms have been described to underlie these two disorders. Despite the accumulating knowledge on this topic, the precise neuropathological mechanisms remain to be elucidated. In this study, we propose that synaptic degeneration plays an important role in the disease progression of depression and AD. Using primary culture of hippocampal neurons treated with oligomeric Aβ and corticosterone as model agents for AD and depression, respectively, we found significant changes in the pre-synaptic vesicle proteins synaptophysin and synaptotagmin. We further investigated whether the observed protein changes affected synaptic functions. By using FM®4-64 fluorescent probe, we showed that synaptic functions were compromised in treated neurons. Our findings led us to investigate the involvement of protein degradation mechanisms in mediating the observed synaptic protein abnormalities, namely, the ubiquitin-proteasome system and autophagy. We found up-regulation of ubiquitin-mediated protein degradation, and the preferential signaling for the autophagic-lysosomal degradation pathway. Lastly, we investigated the neuroprotective role of different classes of antidepressants. Our findings demonstrated that the antidepressants Imipramine and Escitalopram were able to rescue the observed synaptic protein damage. In conclusion, our study shows that synaptic degeneration is an important common denominator underlying depression and AD, and alleviation of this pathology by antidepressants may be therapeutically beneficial.

Abbreviations list

AD – Alzheimer's disease

Aβ – β-amyloid

CORT – Corticosterone

E1 - ubiquitin activating enzymes

E2 – ubiquitin conjugating enzymes

E3 – ubiquitin ligases

HPA – Hypothalamic-pituitary-adrenal

NFT – Neurofibrillary tangles

PSD95 – Post-synaptic density 95

Keywords: Alzheimer's disease; depression; synaptophysin; synaptotagmin; ubiquitin proteasome system; antidepressant

1. Introduction

Alzheimer's disease (AD) is characterized by progressive degeneration of the brain and its functions. As a result, AD patients present with memory deficits, cognitive decline, and diverse behavioral changes [1]. Neuropsychiatric symptoms are observed throughout the course of AD. They occur along the progression of disease and may even occur prior to significant decline in cognitive [2]. Such symptoms include depression, apathy, agitation, and hallucinations. Combined with cognitive deterioration, these symptoms compound patient disability and caregiver burden [3].

AD is represented by two pathological hallmarks, namely β-amyloid (Aβ) plaques and neurofibrillary tangles (NFT). Studies have shown that abnormally folded Aß and tau proteins trigger cascades of neurodegenerative processes, including dysregulation of cholinergic neurons, synaptic degeneration, neuroinflammation, autophagy, and apoptosis [1].

Depression is one of the neuropsychiatric symptoms frequently observed in AD. It is characterized by prolonged period of low mood, anhedonia, and changes in sleep and appetite. Prevalence of depression in AD patients ranges from 20 to 50%. Studies have also shown that depressive symptoms may precede cognitive decline [3, 4].

A number of risk factors for depression in AD patients have been identified: family history of mood disorder in first-degree relatives, past history of depression, female gender, and early onset AD [5, 6]. A history of depression itself has also been associated with increased risks of developing AD, especially among elderly women [5, 7]. Several genetic risk factors have been identified to influence the development of depression and AD, including brain-derived neurotrophic factor genetic variation and being heterozygote for promoter region of interleukin-1β [8, 9].

Several neurobiological mechanisms have been found to cause cellular damage leading to depression. They include hypothalamic-pituitary-adrenal (HPA) axis dysfunction, monoamine deficiency, neuroinflammation, and neuroplastic changes [10]. HPA axis dysfunction appears to be responsible for a great extent of the abnormalities observed in depression. HPA axis dysfunction results in prolonged release of the stress hormone, cortisol, which has been found to be elevated in depressed patients [11]. Cortisol binds to membrane mineralocorticoid and glucocorticoid receptors which allows for rapid modulation of synaptic transmission in the brain [12]. The hippocampus is of particular importance because it is rich in corticosteroid receptors, and structural changes in this brain region has been observed in depressed patients [13].

In the case of AD, high levels of corticotropin-releasing hormone and cortisol, secondary to HPA axis deregulation, have been found to increase the risk and rate of disease progression [14]. Adrenocortical hyperactivity was found to be associated with increased Aβ plaque deposition and NFT formation in an animal model of AD [15].

Furthermore, cholinergic dysfunction found in AD has been shown to suppress glucocorticoid receptor feedback regulation of the HPA axis [16]. Prolonged release of cortisol and HPA axis activation is detrimental to the glucocorticoid-rich hippocampus, which is one of the earliest areas to be affected in AD [17].

It appears that the pathophysiological mechanisms underlying depression are common in AD. For instance, dysregulation of neurotransmitter systems, neuroinflammation and changes in neuroplasticity have been observed in both disorders. Studies are beginning to demonstrate the role of such mechanisms linking depression and AD [18, 19]. We are particularly interested in neuroplastic changes at the synapse, as they are sites of neuronal communication that are essential for proper brain functions. Synaptic plasticity has also been shown to be essential for learning and memory [20].

In AD, altered expressions of synaptic proteins were found to occur early in the disease processes [21] and synaptic degeneration was found to correlate best with cognitive decline [22, 23]. Aβ has been shown to impair synaptic functions and spine structure in animal models of AD [24]. Furthermore, reduction of pre-synaptic vesicle proteins such as synaptophysin has been consistently observed in transgenic AD mouse models [25-27]. In conjunction with loss of pre-synaptic proteins, loss in post-synaptic proteins such as post-synaptic density 95 (PSD95) and glutamate receptor subunit GluR1 has also been demonstrated [28-30].

Synaptic disturbances have also been shown to be involved in several psychiatric disorders, including autism, schizophrenia and bipolar disorder [20, 31]. Evidence suggests altered synaptic structure and functions in depression as well. Loss of hippocampal volume due to reduced neurogenesis has been observed in depressed patients [32, 33]. Reduction in neurogenesis and levels of synaptophysin have been shown in a chronic unpredictable mild stress rat model of depression [34]. In another stressed rat model of depression, dendritic spine loss was observed [35]. Furthermore, over-expression of pre-synaptic protein, piccolo, was found to induce depressive-like behavior in mice [36]. These studies provide evidence that stress is involved in altered synaptic functions, which in turn leads to the development of depression.

Several mechanisms are involved in the disruption of synaptic functions. They include alterations in BDNF and disrupted synaptic signaling pathways responsible for synaptic maturation, impaired synaptic mitochondrial dynamics, and oxidative stress induced variations in synaptic genes [37-39].

Taking into consideration the importance of synapses in maintaining proper brain function and the role of its dysfunction in psychiatric disorders, we hypothesize that synaptic degeneration could be a common link between depression and AD. Since various classes of antidepressants have been the mainstay of depression pharmacotherapy, we also hypothesize that they will be able to ameliorate signs of synaptic damage. This will provide a platform for future drug development to prevent synaptic degeneration in the treatment of depression in AD.

2. Materials and methods

2.1 Cell culture models

Primary culture of hippocampal neurons was used in this study (Supplementary Materials and methods). The hippocampal area was chosen because it is one of the affected areas in both depression and AD. The hippocampus plays important roles in memory consolidation and is one of the earliest affected areas in AD brains [40]. Moreover, the hippocampus contains a large number of glucocorticoid receptors, making it prone to chronic stress, which is highly implicated in depression [41]. Lastly, reduction in hippocampal volume has been observed in both disorders [33, 42].

Oligomeric Aβ1-42 was used as a model agent to represent AD pathologies. Corticosterone (CORT), a rodent derivative of cortisol, was used as a model agent for depression. Both chemicals were used at a sub-lethal dosage to simulate early disease events.

Oligomeric Aβ was reconstituted in anhydrous dimethylsulfoxide (DMSO) (Supplementary Materials and methods) and CORT (Sigma-Aldrich, St. Louis, MO, USA) was reconstituted in 100% ethanol. Both agents were diluted in culture medium to the desired concentration for treatment. The same concentration of anhydrous DMSO or 100% ethanol was diluted in culture medium as control.

To investigate the neuroprotective effects of antidepressants, neurons were pre-treated with Imipramine (Sigma-Aldrich) and Escitalopram (Lundbeck, Copenhagen, Denmark) for 1 hr, and incubated in either oligomeric Aβ or CORT for 24 hr. Imipramine and Escitalopram were dissolved in milliQ water and further diluted in culture medium to the desired concentration for treatment.

2.2 Immunocytochemistry

For immunocytochemical staining, primary hippocampal neurons cultured on coverslips (Thermo Scientific) were fixed with 4% paraformaldehyde (PFA) for 20 min, permeabilized with 0.1% Triton X-100 in TBS for 7 min, and blocked with 10% bovine serum albumin for 1 hr. Incubation of primary antibody was done for 1 hr at room temperature at 1:400 dilution for the following antibodies: synaptophysin (Chemicon, Temecula, CA, USA) and synaptotagmin (Calbiochem, La Jolla, CA, USA). Ubiquitin-48 (Millipore, Billerica, MA, USA), ubiquitin-63 (Millipore), and LC3-II (MBL International, Woburn, MA, USA) were incubated overnight at 4°C at 1:400. Neurons were then incubated with secondary antibody (Anti-rabbit or mouse, Alexa-fluor 488 or 568, 1:400, Molecular Probes, Eugene, OR, USA) and mounted on microscope slides (Thermo Fisher Scientific, Waltham, MA, USA) using ProLong® Gold antifade mounting medium (Invitrogen) and imaged using the LSM510-meta laser scanning confocal microscope (Carl Zeiss, Oberkochen, Germany). Images were analyzed using MacBiophotonics Image J (http://rsb.info.nih.gov/ij/).

2.3 Transduction

Neurons cultured on MatTek dishes were transduced with 10 particles per cell of CellLight® Synaptophysin-GFP (Invitrogen) overnight, prior to treatment. After treatment, neurons were imaged using the LSM510 confocal microscope. Images were then analyzed using MacBiophotonics Image J.

2.4 FM®4-64 fluorescent probe

Five micromolar of FM®4-64 (Invitrogen) fluorescent probe was added to hippocampal neurons cultured on coverslips. The neurons were stimulated with 100 mM potassium chloride for 3 min to induce endocytosis. They were then washed with HBSS and incubated in the dye for 30 min at 37°C and 5% CO_2 for complete endocytosis. One group was fixed with 4% PFA for 20 min. The remaining neurons were then washed and stimulated again with 100 mM potassium chloride for 10 min to induce exocytosis. The second group of neurons was then fixed with 4% PFA for 20 min. The coverslips were mounted on microscope slides using ProLong® Gold antifade mounting medium (Invitrogen), analyzed using the LSM510 confocal microscope and quantified using MacBiophotonics Image J.

2.5 Western blot analysis

Total cell lysate were extracted by ice-cold lysis buffer containing 10 mM Tris (pH 7.4), 100 mM NaCl, 1 mM EDTA, 1mM EGTA, 1 mM NaF, 20 mM $Na_4P_2O_7$, 1% Triton X-100, 10% glycerol, 0.1% SDS, 0.5% deoxycholate, phenylmethylsulfonyl fluoride (1 mM), protease inhibitor cocktail and phosphatase inhibitor cocktail. The lysate was then sonicated, centrifuged at 14,000 rpm for 30 min at 4°C, and the supernatant was collected for analysis. Protein concentration was measured as directed in the protein assay kit (Bio-Rad, Hercules, CA, USA). Protein extracts were separated by SDS-PAGE gel and transferred onto PVDF membrane (Bio-Rad). The membrane was blocked with 5% non-fat milk (Bio-Rad) overnight. Primary antibodies for synaptophysin (Abcam) and synaptotagmin (Abcam) were incubated for 4 hr at 1:2000 dilutions and ß-actin (Sigma) were incubated for 1 hr at 1:5000. Western blots were subsequently incubated with horseradish peroxidase-conjugated secondary antibody for 45 min. Bands were visualized on Biomax X-ray film using ECL spray (Upstate). Bands were quantified using MacBiophotonics Image J.

2.6 Proteasome activity assay

Total cell lysate were harvested with ice cold lysis buffer containing 20 mM Tris, pH 7.2, 1 mM EDTA, 1 mM NaN_3, 1 mM DTT, and protease inhibitor cocktail on ice and centrifuged for 10 min at 20,000 g. Supernatants were quantified in triplicate in black OptiPlate™ 96 well plates (Perkin Elmer, Waltham, USA). Background proteolytic

activity was controlled for by incubation of duplicate samples with 20 μM MG132 (Boston Biochem, Cambridge, MA, USA) prior to incubation with fluorogenic substrates. N-succinyl-Leu-Leu-Val-Tyr-7-amido-4-methylcoumarin (Suc-LLVY-AMC) (Enzo Life Sciences, Farmingdale, USA) for chymotrypsin-like activity, butoxycarbonyl-Leu-Arg-Arg-amido-4-methylcoumarin (Boc-LRR-AMC) (Enzo Life Sciences) for trypsin-like activity, and benzyloxycarbonyl-Leu-Leu-Glu-amido-4-methylcoumarin (Z-LLE-AMC) (Enzo Life Sciences) for caspase-like activity, were incubated with samples at 20 μM for 45 min at 37°C. Fluorescence was read on a microplate reader (Perkin Elmer) at 390 nm excitation and 460 nm emission. Fluorescence activity of all three proteasome proteolytic sites was taken as the level of fluorescence measured after subtraction from background.

2.7 Statistical analysis

Statistical comparison between two groups was determined by unpaired *t*-test. Data for multiple variable comparisons were analyzed by one-way analysis of variance (ANOVA). For the comparison of significance, Tukey's test was used as a *post hoc* test. The statistical program used was GraphPad Prism (GraphPad Software, La Jolla, CA, USA). Results were expressed as mean ± standard error (S.E.) from at least three independent experiments.

3. Results

3.1 Oligomeric Aβ and CORT caused pre-synaptic damage

To investigate the effects of low-dose oligomeric Aβ and CORT on the pre-synaptic site, hippocampal neurons were treated with oligomeric Aβ or CORT at 0.5 μM for 24 hr and immunocytochemical analyses were performed for synaptophysin and synaptotagmin. Primary hippocampal neurons were also transduced with CellLight® Synaptophysin-GFP for live-cell imaging. The number of immunoreactive positive puncta of synaptophysin and synaptotagmin was reduced after 24 hr of Aβ treatment (Fig. 1 A-E). Aggregation of synaptophysin and synaptotagmin was observed after treatment with 0.5 μM Aβ for 12 hr (Fig. 1 A, F & G). Protein expression of synaptophysin and synaptotagmin was reduced with 0.5 and 5 μM Aβ treatment by western blot analysis (Fig. 1 H-J). CORT induced aggregation of the synaptic proteins (Fig. 2 A-D), without affecting the total protein expression level (Fig. 2 E & F).

3.2 Oligomeric Aβ and CORT compromised synaptic functions

To investigate whether the observed pathological changes affected synaptic functions, we employed the FM®4-64 fluorescent probe, which is commonly used to examine endocytosis and exocytosis. Endocytosis is monitored by dye uptake and the subsequent increase in fluorescent intensity. Exocytosis is examined by dye release and the subsequent decrease in fluorescent intensity. Images shown in the figure represent

dye uptake and release specifically at the neuritis (Fig. 3). Oligomeric Aβ and CORT treatment at 0.5 μM showed similar fluorescent intensities compared to control during dye uptake, indicating that endocytosis was unaffected (Fig. 3 A & B). However, during exocytosis when the dye was supposed to be released (and the subsequent decrease in fluorescent intensity), the fluorescent intensity of the treated neurons remained at a high level (Fig. 3 A & C), suggesting an impairment in exocytosis following oligomeric Aβ and CORT treatment.

3.3 Involvement of protein degradation mechanisms at the synapse

Since our results showed loss and aggregations of synaptic protein, we further investigated the mechanisms underlying the clearance of aggregated synaptic proteins. We found that oligomeric Aβ and CORT at 0.5 μM influenced ubiquitin-mediated protein degradation mechanisms, indicated by the increase in the immunoreactivity of ubiquitin-48 and ubiquitin-63 (Fig. 4 A & B, D & E). Ubiquitin-63 was found to significantly co-localize with synaptophysin (Fig. 4 D & F). On the other hand, ubiquitin-48 was found in close proximity to synaptophysin, but did not significantly co-localize (Fig. 4 A & C). Lactacystin, a proteasome inhibitor, served as a positive control for ubiquitin accumulation.

3.4 Corticosterone and oligomeric Aβ did not affect proteasome activity

Since oligomeric Aβ and CORT were found to induce an increased co-localization between synaptophysin with ubiquitin-63 but not with ubiquitin-48, the ubiquitin-proteasome pathway may not be the major pathway or mechanism being affected in oligomeric Aβ- and CORT-treated cells. Therefore, we went on to examine whether oligomeric Aβ and CORT treatment affect proteasome activity within our model. Our results found no significant changes in the chymotrypsin-like, trypsin-like and caspase-like activity of the proteasome in both treatment groups (Fig. 5).

3.5 Antidepressants were able to alleviate pathological changes of pre-synaptic proteins

Antidepressants that target the monoaminergic system have long been used in the treatment of major depressive disorder. Therefore, we investigated if they could alleviate the pre-synaptic damage exerted by oligomeric Aβ and CORT treatment. Results demonstrated that pre-treatment with 10 μM Imipramine or Escitalopram for 1 hr was able to rescue the observed synaptic pathologies (Fig. 6). For oligomeric Aβ treated cells, immunofluorescent analysis of synaptophysin and synaptotagmin showed a significant increase in the number of positive puncta after pre-treatment with antidepressants (Fig. 6 A-C). Pre-treatment with Imipramine or Escitalopram was able to reduce the number of synaptic protein aggregations in CORT-treated neurons (Fig.6 D-F).

4. Discussions

Depression and AD share common pathophysiological characteristics including synaptic degeneration [43]. Synaptic degeneration is reflected by pathological changes within the molecular components of pre- and post-synaptic compartments [20]. Our results showed damages in the pre-synaptic compartment, which was found to affect the recycling of synaptic vesicles and ultimately the function of the synapse. Next, we found that ubiquitin-mediated protein degradation mechanisms appeared to be responsible for the clearance of aggregated synaptic proteins, which may mediate the degenerative processes. Furthermore, we found that antidepressants were able to alleviate the observed pre-synaptic damage.

4.1 Synaptic damage

Our results showed the pre-synaptic compartment was damaged after treatment with oligomeric Aβ and CORT. Pre-synaptic protein aggregation was observed after 12 hr of treatment with Aβ, and protein loss was observed at 24 hr (Fig. 1). Although these changes were present, the dosage used did not significantly affect cell viability or induce apoptosis (Supplementary Fig. 1& 2). With CORT, pre-synaptic protein aggregation but not protein loss was observed 24 hr after treatment (Fig. 2). These observations suggest that pre-synaptic proteins undergo aggregation, followed by loss of proteins. Since there was no significant change in PSD95 following treatment with Aβ and CORT (Supplementary Fig. 3&4), it appeared that pre-synaptic damage occurred before post-

synaptic damage. There is a possibility that PSD95 could be affected after 24 hr; however, longer treatment durations were not investigated. Despite the temporal differences in the occurrence of the synaptic pathologies, the pre-synaptic damage induced by CORT resembled that induced by oligomeric Aβ.

Our next question was whether the observed morphological changes would affect synaptic functions. Synaptic vesicles undergo trafficking, docking, fusion to the synaptic membrane, and ultimately the release of neurotransmitters. After neurotransmitter release, empty synaptic vesicles either recycles back to the releasable pool or fuses with the endosome where mature vesicles subsequently bud off [44]. The FM®4-64 fluorescent probe is commonly used to label synaptic vesicles for live-cell imaging of synaptic function [45]. Upon neuronal stimulation, the synaptic vesicles will release the dye through exocytosis. The decrease in dye intensity over a period of time indicates the rate of exocytosis. Our results showed that after treatment with oligomeric Aβ and CORT, dye exocytosis was slower (Fig. 3). These results indicate that the observed pathological changes affect synaptic functions by delaying exocytosis and perhaps the release of neurotransmitters.

4.2 Protein degradation and the synapse

To further elucidate the mechanisms underlying the synaptic protein damages, protein degradation mechanisms were investigated. The major cellular protein degradation pathways are the ubiquitin-proteasome system and the autophagy-lysosomal

pathway. Ubiquitin appears to be a common denominator in targeting unwanted proteins for degradation by both pathways. Also, ubiquitinated proteins are consistently present in protein aggregates found in many neurodegenerative diseases [46].

Ubiquitination involves a cascade of enzymes including ubiquitin-activating enzymes (E1), conjugating enzymes (E2), and ligases (E3) [47]. E1 binds to ubiquitin and ATP to form a complex. Ubiquitin is then passed on to E2. Ubiquitin-charged E2 then forms a complex with an E3 ligase and a protein substrate. Ubiquitin is then transferred onto the protein substrate. Studies have shown that if the protein substrate is linked to the lysine 48 residue of ubiquitin, the substrate is signaled for degradation by the proteasome. On the other hand, if the polyubiquitin chain is formed by the linkage of the substrate to the lysine 63 residue, the substrate is preferentially degraded by the lysosome[48].

Our results showed that there was an increase in ubiquitin-48 and -63 immunoreactivities in both Aβ and CORT treated groups (Fig. 4). At the synaptic level, our findings support previous studies that investigate the crucial involvement of protein degradation mechanisms in maintaining proper synaptic functions. Ubiquitin has been known to function locally at the synapse [49] and several ubiquitin related enzymes have been found to regulate synaptic functions [50]. Furthermore, several synaptic proteins are substrates for ubiquitin, including synaptophysin [51].

Our results also showed that ubiquitin-63 significantly co-localized with synaptophysin for both treatment groups, while ubiquitin-48 did not (Fig. 4). Pathological

accumulation of autophagic vacuoles has been observed in AD brains [52, 53]. Up-regulation of the autophagy-lysosomal degradation pathway has been shown to increase production and accumulation of intracellular Aβ [54]. Our observations suggest that up-regulation of this degradation pathway is also associated with CORT induced toxicity, providing another evidence for the similarities between depression and AD.

Higher levels of co-localization between ubiquitin-63 and synaptophysin after treatment with Aβ and CORT would suggest increased activation of ubiquitin-mediated protein degradation that preferentially signals for autophagy-lysosomal degradation pathway. Treatment with CORT or Aβ did not induce changes in any of the three proteolytic activities of the proteasome (Fig. 5), supporting the notion that following treatment, the autophagy-lysosomal pathway may play a more prominent role compared to the ubiquitin-proteasome pathway.

To further elucidate the activation of the autophagic pathway, we performed immunocytochemical analysis for LC3-II, which is a marker for autophagosomes [55] (Supplementary Fig. 5). LC3-II is a protein located on the inner and outer membrane of autophagosomes. Ubiquitinated proteins at lysine 63 recruit the LC3-interacting protein p62. p62 is then recognized by LC3-II. Protein substrate tagged with ubiquitin-63, p62 and LC3-II forms a complex which is then engulfed by the autophagosome, and subsequently degraded by the lysosomes [56]. In accordance with the increased immunoreactivity of ubiquitin-63 in Aβ and CORT treated cells, there was also an increase in the number of LC3-II puncta following treatment. Therefore, in our study, we

demonstrated that increased activation of the ubiquitin-mediated autophagy-lysosomal degradation pathway induced by either CORT or Aβ, which may contribute to the pathological changes in pre-synaptic proteins and its functions.

The role of protein degradation at the synapse is to maintain its plasticity; however, the imbalance in the degradation process may disturb synaptic functions [57]. Protein degradation mechanisms are important in maintaining proper synaptic function and its dysfunction could have detrimental results in the synapse. Although the involvement of ubiquitinated proteins and autophagy has been widely investigated in AD pathology, it is not well studied in depression. This study suggests the possible importance of its role in the pathology of depression. Since modulation of the autophagy-lysosomal protein degradation pathway has been shown to lead to numerous neurodegenerative diseases, its involvement in depression provides new insight as to why depressed patients may develop neurodegenerative diseases such as AD later on in life.

4.3 Antidepressants are able to alleviate pre-synaptic protein damages

According to our findings, synaptic degeneration may be an upstream pathological process in depression in AD. Our results demonstrated that the selected antidepressants were able to alleviate the observed synaptic damage. The use of various antidepressants have long been used in treating depressive disorders [58]. Several classes of antidepressants are available, including tricyclic antidepressants (TCA) and the selective serotonin reuptake inhibitors (SSRI) [59, 60]. Several studies have shown that

SSRIs are able to improve cognition and depressive symptoms in both animal models and AD patients [5, 61, 62]. However, a recent clinical trial of the SSRI Sertraline, and the noradrenergic and specific serotonergic antidepressant Mirtazapine failed to show any effects over placebo in the treatment of depression in AD patients [63].

We selected one of the "classical" TCA Imipramine and the newer SSRI Escitalopram for our study to investigate whether these antidepressants would be able to protect neurons from the toxic effects induced by Aβ and CORT. Our study showed that both antidepressants could attenuate the loss or aggregation of synaptic proteins (Fig. 6). Interestingly, Imipramine and Escitalopram are two different classes of antidepressants, with Imipramine being non-specific, while Escitalopram being highly specific to the serotonergic system. This suggests that the modulation of serotonin uptake transporters may not be the only underlying mechanism involved. It would be interesting to further investigate other possible underlying pathways of how antidepressant affects synaptic proteins.

It is important to note that the pathogenesis of depression and AD does not only involve synaptic degeneration. Although the present study has shown that synaptic degeneration and ubiquitin-mediated protein degradation mechanisms are involved in depression and AD, other factors including neuroinflammation, oxidative stress, and neurotransmitter dysregulation cannot be excluded. Since we have utilized an *in vitro* disease model for this study, we were only able to investigate the effects of CORT as a model for depression and oligomeric Aβ as a model for AD. Other factors involved in

each disorder were not investigated including monoamine deficiency for depression and NFT for AD.

Depression appears to share similar neurodegenerative processes as AD. We have provided significant evidence to show that synaptic degeneration is a common pathological feature of both depression and AD. The observed synaptic protein loss and aggregation appeared to be associated with the ubiquitin-mediated autophagy-lysosomal pathway. Since the involvement of this pathway is not well studied in depression, our study provides new insight into the pathology of depression and further supports the idea that similar molecular neuropathology exists between depression and AD. Moreover, our observation that antidepressants were able to alleviate the synaptic pathologies, implicates that the prevention of synaptic degeneration may be pivotal in the early therapeutic intervention of these two disorders and further investigations are highly warranted.

Acknowledgement:

The work was partially supported by University Seed Funding for Basic Science Research (201211159058 & 201022259118), The University of Hong Kong Alzheimer's Disease Research Network under University Strategic Research Theme on Healthy Aging, generous support from Ms Kit-Wan Chow.

Figure legends

Figure 1. Low-dose oligomeric Aβ induced aggregation of pre-synaptic proteins at 12 hr and loss of pre-synaptic proteins at 24 hr. A & D) Treatment with 0.5 μM Aβ for 24 hr caused a reduction in the number of immunoreactive puncta of synaptophysin and synaptotagmin while aggregations of these proteins were observed after 12 hr treatment. Live-cell imaging of primary hippocampal neurons transduced with CellLight® Synaptophysin-GFP also showed reduction in immunoreactive positive puncta. Images were taken at 63x objective (scale bar 10 μm) B,C,E,F,G). Quantitative analysis of the number of puncta and aggregations was performed by MacBiophotonics Image J. Results were expressed as fold of control ± SE from at least 3 independent experiments. Statistical analysis was performed by unpaired *t*-test. * represents $p<0.05$ compared to the corresponding control. H) Western-blot analysis of pre-synaptic proteins showed reduced protein levels. I) Quantitative analysis of western blot by MacBiophotonics Image J. Results were expressed as fold of control ± SE from at least 3 independent experiments. Statistical analysis was performed by one-way ANOVA, followed by the *post hoc* Tukey's test. * represents $p<0.05$ compared to the corresponding control.

Figure 2. Low-dose CORT induced aggregation of pre-synaptic proteins. A) Staining for synaptotagmin and synaptophysin showed that treatment with 0.5 μM CORT for 24 hr induced protein aggregations. Live-cell imaging of primary hippocampal neurons transduced with CellLight® Synaptophysin-GFP also showed pre-synaptic protein aggregations under the same conditions. Images were taken at 63x objective (scale bar 10

μm). B-D) Quantitative analysis of the immunoreactivity was performed by MacBiophotonics Image J. The amount of aggregation of synaptophysin and synaptotagmin after treatment was found to be significantly increased. Aggregations were defined by size of the puncta over number of puncta. Results were expressed as fold of control ± SE from at least 3 independent experiments. Statistical analysis was performed by unpaired *t*-test. * represents $p<0.05$ compared to the corresponding control. E) Western-blot analysis showed no change in protein expression levels of synaptic proteins after treatment with 0.5 and 5 μM CORT for 24 hr. F) Quantitative analysis of Western-blot was performed by MacBiophotonics Image J. Results were expressed as fold of control ± SE from at least 3 independent experiments. Statistical analysis was performed by one-way ANOVA, followed by the *post hoc* Tukey's test.

Figure 3. Low-dose oligomeric Aβ and CORT slowed down FM®4-64 dye release, hence exocytosis. A) FM®4-64 dye was used to investigate endocytosis (dye uptake, increase in fluorescent intensity) and exocytosis (dye release, decrease in fluorescent intensity). Images shown represent dye uptake and release specifically at the neurites. B) MacBiophotonics Image J was used to quantify the fluorescent intensities of FM®4-64 dye. Results showed similar fluorescent intensities during dye uptake, indicating that endocytosis was unaffected. However, during exocytosis when the dye was supposed to be released (and the subsequent decrease in fluorescent intensity), C) fluorescent intensity of the treated neurons remained at an elevated level. This indicates that the fluorescent probe was not being properly released; hence exocytosis appeared to be slower in treated neurons. Results were expressed as fold of control ± SE from at least 3 independent

experiments. Statistical analysis was performed by unpaired *t*-test. * & ** represent $p<0.05$ and $p<0.01$ compared to the corresponding control. Images were taken at 63x objective (3x digital zoom; scale bar 10 μm).

Figure 4. Low-dose oligomeric Aβ and CORT induced ubiquitin-mediated protein degradation mechanisms. A) Primary hippocampal neurons were examined for synaptophysin and ubiquitin-48 immunoreactivity. Increase in the number of positive ubiquitin-48 puncta and co-localization with synaptophysin (indicated by arrows) was observed. Lactacystin at 10 μM served as a positive control. B) Quantification of the immunoreactivity was performed by MacBiophotonics Image J. There was a significant increase in number of puncta after treatment. Results were expressed as fold of control ± SE from at least 3 independent experiments. Statistical analysis was performed by one-way ANOVA, followed by the *post hoc* Tukey's test. *, **, & *** represent $p<0.05$, $p<0.01$, and $p<0.001$compared to the corresponding control. C) Mander's coefficient for co-localization analysis showed no significant increase in the co-localization level in the treated group, except in the lactacystin treated neurons. Statistical analysis was performed by one-way ANOVA, followed by the *post hoc* Tukey's test. * represents $p<0.05$ compared to the corresponding control. D) Primary hippocampal neurons were examined for synaptophysin and ubiquitin-63 immunoreactivity. Increase in the number of ubiquitin-63 puncta and co-localization with synaptophysin (indicated by arrows) was observed. Lactacystin-treated cells served as a positive control. E) Quantification of the immunoreactivity was performed by MacBiophotonics Image J. There was a significant increase in number of puncta after treatment. Results were expressed as fold of control ±

SE from at least 3 independent experiments. Statistical analysis was performed by one-way ANOVA, followed by the *post hoc* Tukey's test. *, **, & *** represents $p<0.05$, $p<0.01$, and $p<0.001$ compared to the corresponding control. F) Mander's coefficient for co-localization analysis showed a significant increase in the co-localization level of synaptophysin and ubiquitin-63 in the treated group. Statistical analysis was performed by one-way ANOVA, followed by the *post hoc* Tukey's test. *, **, & *** represent $p<0.05$, $p<0.01$, and $p<0.001$, respectively, compared to the corresponding control. Images were taken at 63x objective (3x digital zoom; scale bar 10 μm).

Figure 5. Low-dose oligomeric Aβ and CORT did not mediate changes in proteasome activity. Primary hippocampal neurons were treated with 0.5μM Aβ and CORT and analysed for proteasome activity using a fluorescence activity assay. No significant changes in the chymotrypsin-like, trypsin-like, and caspase-like activities of the proteasome were found after treatment with low dose oligomeric Aβ and CORT. Results were expressed as fold of control ± SE from 4 independent experiments. Statistical analysis was performed by one-way ANOVA followed by the *post hoc* Tukey's test.

Figure 6. A) Antidepressants Imipramine and Escitalopram were able to alleviate the observed synaptic pathologies after low-dose oligomeric Aβ treatment. Primary hippocampal neurons were pre-treated for 1 hr with Imipramine or Escitalopram. Immunostaining of synaptophysin and synaptotagmin showed an increase in number of puncta. Plus signs indicate antidepressant pre-treatment followed by oligomeric Aβ treatment. B&C) Quantification of immunostaining was performed by MacBiophotonics

Image J. Results showed that the number of puncta increased significantly after Aβ treatment. Results were expressed as fold of control ± SE from at least 3 independent experiments. Statistical analysis was performed by one-way ANOVA followed by the *post hoc* Tukey's test. * represents $p<0.05$ compared to 0.5 μM Aβ. D) Antidepressants Imipramine and Escitalopram were able to alleviate the observed synaptic pathologies after low-dose CORT treatment. Primary hippocampal neurons were pre-treated for 1 hr with Imipramine or Escitalopram. Immunofluorescent analysis of synaptophysin and synaptotagmin showed a reduction in protein aggregation. Plus signs indicate antidepressant pre-treatment followed by CORT treatment. E &F) Quantification of immunostaining was performed by MacBiophotonics Image J. Results showed that the number of aggregations was significantly reduced after CORT treatment. Results were expressed as fold of control ± SE from at least 3 independent experiments. Statistical analysis was performed by one-way ANOVA followed by the *post hoc* Tukey's test. * represents $p<0.05$ compared to 0.5 μM CORT. Images were taken at 63x objective (scale bar 10 μm).

References

[1] M. Goedert, M.G. Spillantini, A century of Alzheimer's disease, Science, 314 (2006) 777-781.
[2] W.C. Chan, L.C. Lam, C.W. Tam, V.W. Lui, G.T. Leung, A.T. Lee, S.S. Chan, A.W. Fung, H.F. Chiu, W.M. Chan, Neuropsychiatric symptoms are associated with increased risks of progression to dementia: a 2-year prospective study of 321 Chinese older persons with mild cognitive impairment, Age Ageing, 40 (2011) 30-35.
[3] S. Gauthier, J. Cummings, C. Ballard, H. Brodaty, G. Grossberg, P. Robert, C. Lyketsos, Management of behavioral problems in Alzheimer's disease, Int Psychogeriatr, 22 (2010) 346-372.
[4] D. Enache, B. Winblad, D. Aarsland, Depression in dementia: epidemiology, mechanisms, and treatment, Curr Opin Psychiatry, 24 (2011) 461-472.
[5] C.G. Lyketsos, J. Olin, Depression in Alzheimer's disease: overview and treatment, Biol Psychiatry, 52 (2002) 243-252.
[6] Z.A. Butt, M.E. Strauss, Relationship of family and personal history to the occurrence of depression in persons with Alzheimer's disease, Am J Geriatr Psychiatry, 9 (2001) 249-254.
[7] R.C. Green, L.A. Cupples, A. Kurz, S. Auerbach, R. Go, D. Sadovnick, R. Duara, W.A. Kukull, H. Chui, T. Edeki, P.A. Griffith, R.P. Friedland, D. Bachman, L. Farrer, Depression as a risk factor for Alzheimer disease: the MIRAGE Study, Arch Neurol, 60 (2003) 753-759.
[8] M.C. McCulley, I.N. Day, C. Holmes, Association between interleukin 1-beta promoter (-511) polymorphism and depressive symptoms in Alzheimer's disease, Am J Med Genet B Neuropsychiatr Genet, 124B (2004) 50-53.
[9] B. Borroni, S. Archetti, C. Costanzi, M. Grassi, M. Ferrari, A. Radeghieri, L. Caimi, C. Caltagirone, M. Di Luca, A. Padovani, Role of BDNF Val66Met functional polymorphism in Alzheimer's disease-related depression, Neurobiol Aging, 30 (2009) 1406-1412.
[10] V. Krishnan, E.J. Nestler, The molecular neurobiology of depression, Nature, 455 (2008) 894-902.
[11] C.M. Pariante, S.L. Lightman, The HPA axis in major depression: classical theories and new developments, Trends Neurosci, 31 (2008) 464-468.
[12] S. Moylan, M. Maes, N.R. Wray, M. Berk, The neuroprogressive nature of major depressive disorder: pathways to disease evolution and resistance, and therapeutic implications, Mol Psychiatry, 18 (2013) 595-606.
[13] E. Palazidou, The neurobiology of depression, Br Med Bull, 101 (2012) 127-145.
[14] G. Murialdo, F. Nobili, A. Rollero, M.V. Gianelli, F. Copello, G. Rodriguez, A. Polleri, Hippocampal perfusion and pituitary-adrenal axis in Alzheimer's disease, Neuropsychobiology, 42 (2000) 51-57.
[15] K.N. Green, L.M. Billings, B. Roozendaal, J.L. McGaugh, F.M. LaFerla, Glucocorticoids increase amyloid-beta and tau pathology in a mouse model of Alzheimer's disease, J Neurosci, 26 (2006) 9047-9056.
[16] K.A. Helm, D.R. Ziegler, M. Gallagher, Habituation to stress and dexamethasone suppression in rats with selective basal forebrain cholinergic lesions, Hippocampus, 14 (2004) 628-635.

[17] S. Aznar, G.M. Knudsen, Depression and Alzheimer's disease: is stress the initiating factor in a common neuropathological cascade?, J Alzheimers Dis, 23 (2011) 177-193.
[18] A. Briones, S. Gagno, E. Martisova, M. Dobarro, B. Aisa, M. Solas, R. Tordera, M. Ramirez, Stress-induced anhedonia is associated with an increase in Alzheimer's disease-related markers, Br J Pharmacol, 165 (2012) 897-907.
[19] M. Maes, M. Kubera, E. Obuchowiczwa, L. Goehler, J. Brzeszcz, Depression's multiple comorbidities explained by (neuro)inflammatory and oxidative & nitrosative stress pathways, Neuro Endocrinol Lett, 32 (2011) 7-24.
[20] C.L. Waites, C.C. Garner, Presynaptic function in health and disease, Trends Neurosci, 34 (2011) 326-337.
[21] E. Masliah, M. Mallory, M. Alford, R. DeTeresa, L.A. Hansen, D.W. McKeel, Jr., J.C. Morris, Altered expression of synaptic proteins occurs early during progression of Alzheimer's disease, Neurology, 56 (2001) 127-129.
[22] S.T. DeKosky, S.W. Scheff, S.D. Styren, Structural correlates of cognition in dementia: quantification and assessment of synapse change, Neurodegeneration, 5 (1996) 417-421.
[23] T. Ma, E. Klann, Amyloid beta: linking synaptic plasticity failure to memory disruption in Alzheimer's disease, J Neurochem, 120 Suppl 1 (2012) 140-148.
[24] G.M. Shankar, S. Li, T.H. Mehta, A. Garcia-Munoz, N.E. Shepardson, I. Smith, F.M. Brett, M.A. Farrell, M.J. Rowan, C.A. Lemere, C.M. Regan, D.M. Walsh, B.L. Sabatini, D.J. Selkoe, Amyloid-beta protein dimers isolated directly from Alzheimer's brains impair synaptic plasticity and memory, Nat Med, 14 (2008) 837-842.
[25] W.G. Honer, Pathology of presynaptic proteins in Alzheimer's disease: more than simple loss of terminals, Neurobiol Aging, 24 (2003) 1047-1062.
[26] D. Tampellini, E. Capetillo-Zarate, M. Dumont, Z. Huang, F. Yu, M.T. Lin, G.K. Gouras, Effects of synaptic modulation on beta-amyloid, synaptophysin, and memory performance in Alzheimer's disease transgenic mice, J Neurosci, 30 (2010) 14299-14304.
[27] T. Spires-Jones, S. Knafo, Spines, plasticity, and cognition in Alzheimer's model mice, Neural Plast, 2012 (2012) 319836.
[28] C.G. Almeida, D. Tampellini, R.H. Takahashi, P. Greengard, M.T. Lin, E.M. Snyder, G.K. Gouras, Beta-amyloid accumulation in APP mutant neurons reduces PSD-95 and GluR1 in synapses, Neurobiol Dis, 20 (2005) 187-198.
[29] R. Sultana, W.A. Banks, D.A. Butterfield, Decreased levels of PSD95 and two associated proteins and increased levels of BCl2 and caspase 3 in hippocampus from subjects with amnestic mild cognitive impairment: Insights into their potential roles for loss of synapses and memory, accumulation of Abeta, and neurodegeneration in a prodromal stage of Alzheimer's disease, J Neurosci Res, 88 (2010) 469-477.
[30] R.M. Koffie, M. Meyer-Luehmann, T. Hashimoto, K.W. Adams, M.L. Mielke, M. Garcia-Alloza, K.D. Micheva, S.J. Smith, M.L. Kim, V.M. Lee, B.T. Hyman, T.L. Spires-Jones, Oligomeric amyloid beta associates with postsynaptic densities and correlates with excitatory synapse loss near senile plaques, Proc Natl Acad Sci U S A, 106 (2009) 4012-4017.
[31] G. Gonzalez-Burgos, K.N. Fish, D.A. Lewis, GABA neuron alterations, cortical circuit dysfunction and cognitive deficits in schizophrenia, Neural Plast, 2011 (2011) 723184.

[32] B. Czeh, P.J. Lucassen, What causes the hippocampal volume decrease in depression? Are neurogenesis, glial changes and apoptosis implicated?, Eur Arch Psychiatry Clin Neurosci, 257 (2007) 250-260.
[33] A. Neumeister, S. Wood, O. Bonne, A.C. Nugent, D.A. Luckenbaugh, T. Young, E.E. Bain, D.S. Charney, W.C. Drevets, Reduced hippocampal volume in unmedicated, remitted patients with major depression versus control subjects, Biol Psychiatry, 57 (2005) 935-937.
[34] D. Yang, Q. Li, L. Fang, K. Cheng, R. Zhang, P. Zheng, Q. Zhan, Z. Qi, S. Zhong, P. Xie, Reduced neurogenesis and pre-synaptic dysfunction in the olfactory bulb of a rat model of depression, Neuroscience, 192 (2011) 609-618.
[35] T. Hajszan, A. Dow, J.L. Warner-Schmidt, K. Szigeti-Buck, N.L. Sallam, A. Parducz, C. Leranth, R.S. Duman, Remodeling of hippocampal spine synapses in the rat learned helplessness model of depression, Biol Psychiatry, 65 (2009) 392-400.
[36] Y. Furukawa-Hibi, A. Nitta, H. Fukumitsu, H. Somiya, S. Furukawa, T. Nabeshima, K. Yamada, Overexpression of piccolo C2A domain induces depression-like behavior in mice, Neuroreport, 21 (2010) 1177-1181.
[37] R.S. Duman, G.K. Aghajanian, Synaptic dysfunction in depression: potential therapeutic targets, Science, 338 (2012) 68-72.
[38] P.H. Reddy, R. Tripathi, Q. Troung, K. Tirumala, T.P. Reddy, V. Anekonda, U.P. Shirendeb, M.J. Calkins, A.P. Reddy, P. Mao, M. Manczak, Abnormal mitochondrial dynamics and synaptic degeneration as early events in Alzheimer's disease: implications to mitochondria-targeted antioxidant therapeutics, Biochim Biophys Acta, 1822 (2012) 639-649.
[39] D.A. Forero, G. Casadesus, G. Perry, H. Arboleda, Synaptic dysfunction and oxidative stress in Alzheimer's disease: emerging mechanisms, J Cell Mol Med, 10 (2006) 796-805.
[40] H. Hampel, K. Burger, S.J. Teipel, A.L. Bokde, H. Zetterberg, K. Blennow, Core candidate neurochemical and imaging biomarkers of Alzheimer's disease, Alzheimers Dement, 4 (2008) 38-48.
[41] M. Joels, Functional actions of corticosteroids in the hippocampus, Eur J Pharmacol, 583 (2008) 312-321.
[42] E. Geuze, E. Vermetten, J.D. Bremner, MR-based in vivo hippocampal volumetrics: 2. Findings in neuropsychiatric disorders, Mol Psychiatry, 10 (2005) 160-184.
[43] S. Wuwongse, R.C. Chang, A.C. Law, The putative neurodegenerative links between depression and Alzheimer's disease, Prog Neurobiol, 91 (2010) 362-375.
[44] J. Richmond, Synaptic function, WormBook, 30 (2005) 1-14.
[45] M.A. Gaffield, W.J. Betz, Imaging synaptic vesicle exocytosis and endocytosis with FM dyes, Nat Protoc, 1 (2006) 2916-2921.
[46] M.J. Clague, S. Urbe, Ubiquitin: same molecule, different degradation pathways, Cell, 143 (2010) 682-685.
[47] A. Ciechanover, The ubiquitin proteolytic system: from a vague idea, through basic mechanisms, and onto human diseases and drug targeting, Neurology, 66 (2006) S7-19.
[48] H. Wu, Y.C. Lo, S.C. Lin, Recent advances in polyubiquitin chain recognition, F1000 Biol Rep, 2 (2010) 1-5.

[49] S.D. Speese, N. Trotta, C.K. Rodesch, B. Aravamudan, K. Broadie, The ubiquitin proteasome system acutely regulates presynaptic protein turnover and synaptic efficacy, Curr Biol, 13 (2003) 899-910.
[50] B. Bingol, M. Sheng, Deconstruction for reconstruction: the role of proteolysis in neural plasticity and disease, Neuron, 69 (2011) 22-32.
[51] T.C. Wheeler, L.S. Chin, Y. Li, F.L. Roudabush, L. Li, Regulation of synaptophysin degradation by mammalian homologues of seven in absentia, J Biol Chem, 277 (2002) 10273-10282.
[52] D.C. Rubinsztein, The roles of intracellular protein-degradation pathways in neurodegeneration, Nature, 443 (2006) 780-786.
[53] B. Levine, G. Kroemer, Autophagy in the pathogenesis of disease, Cell, 132 (2008) 27-42.
[54] L.M. Billings, S. Oddo, K.N. Green, J.L. McGaugh, F.M. LaFerla, Intraneuronal Abeta causes the onset of early Alzheimer's disease-related cognitive deficits in transgenic mice, Neuron, 45 (2005) 675-688.
[55] N. Mizushima, T. Yoshimori, B. Levine, Methods in mammalian autophagy research, Cell, 140 313-326.
[56] Y. Ichimura, M. Komatsu, Selective degradation of p62 by autophagy, Semin Immunopathol, 32 431-436.
[57] A.N. Hegde, The ubiquitin-proteasome pathway and synaptic plasticity, Learn Mem, 17 (2010) 314-327.
[58] E. Tedeschini, Y. Levkovitz, N. Iovieno, V.E. Ameral, J.C. Nelson, G.I. Papakostas, Efficacy of antidepressants for late-life depression: a meta-analysis and meta-regression of placebo-controlled randomized trials, J Clin Psychiatry, 72 (2011) 1660-1668.
[59] R. Kuhn, The treatment of depressive states with G 22355 (imipramine hydrochloride), Am J Psychiatry, 115 (1958) 459-464.
[60] J. Undurraga, R.J. Baldessarini, Randomized, Placebo-Controlled Trials of Antidepressants for Acute Major Depression: Thirty-Year Meta-Analytic Review, Neuropsychopharmacology, 37 (2011) 851-864.
[61] E. Mossello, M. Boncinelli, V. Caleri, M.C. Cavallini, E. Palermo, M. Di Bari, S. Tilli, E. Sarcone, D. Simoni, C.A. Biagini, G. Masotti, N. Marchionni, Is antidepressant treatment associated with reduced cognitive decline in Alzheimer's disease?, Dement Geriatr Cogn Disord, 25 (2008) 372-379.
[62] R.L. Nelson, Z. Guo, V.M. Halagappa, M. Pearson, A.J. Gray, Y. Matsuoka, M. Brown, B. Martin, T. Iyun, S. Maudsley, R.F. Clark, M.P. Mattson, Prophylactic treatment with paroxetine ameliorates behavioral deficits and retards the development of amyloid and tau pathologies in 3xTgAD mice, Exp Neurol, 205 (2007) 166-176.
[63] S. Banerjee, J. Hellier, M. Dewey, R. Romeo, C. Ballard, R. Baldwin, P. Bentham, C. Fox, C. Holmes, C. Katona, M. Knapp, C. Lawton, J. Lindesay, G. Livingston, N. McCrae, E. Moniz-Cook, J. Murray, S. Nurock, M. Orrell, J. O'Brien, M. Poppe, A. Thomas, R. Walwyn, K. Wilson, A. Burns, Sertraline or mirtazapine for depression in dementia (HTA-SADD): a randomised, multicentre, double-blind, placebo-controlled trial, Lancet, 378 (2011) 403-411.

Figure

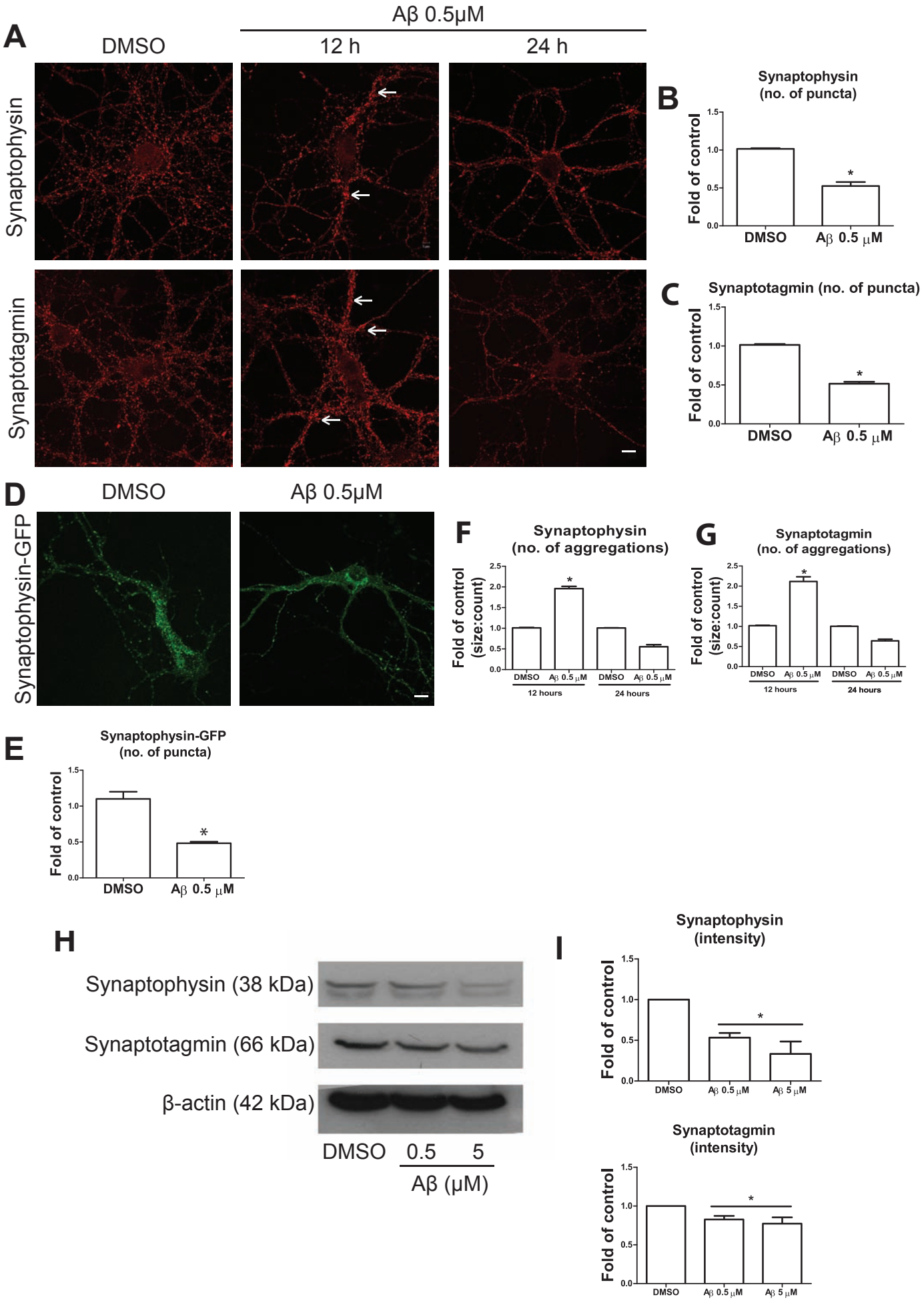

Fig. 1

Wuwongse et al., 2013

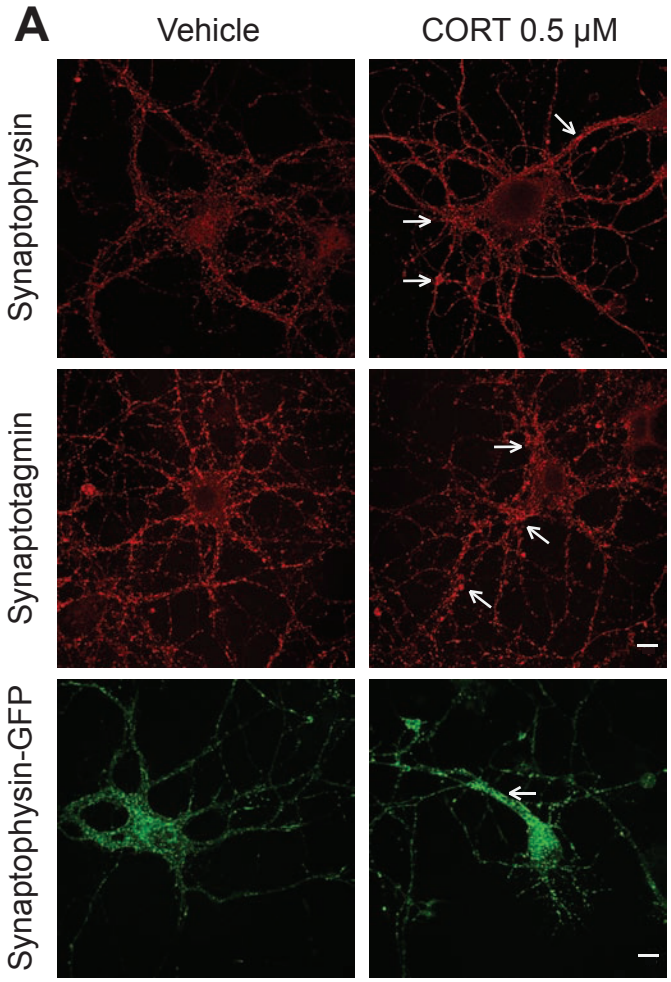

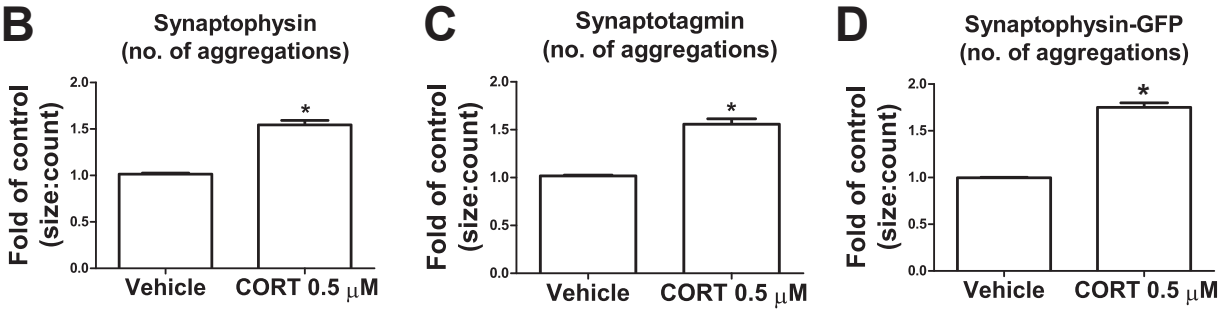

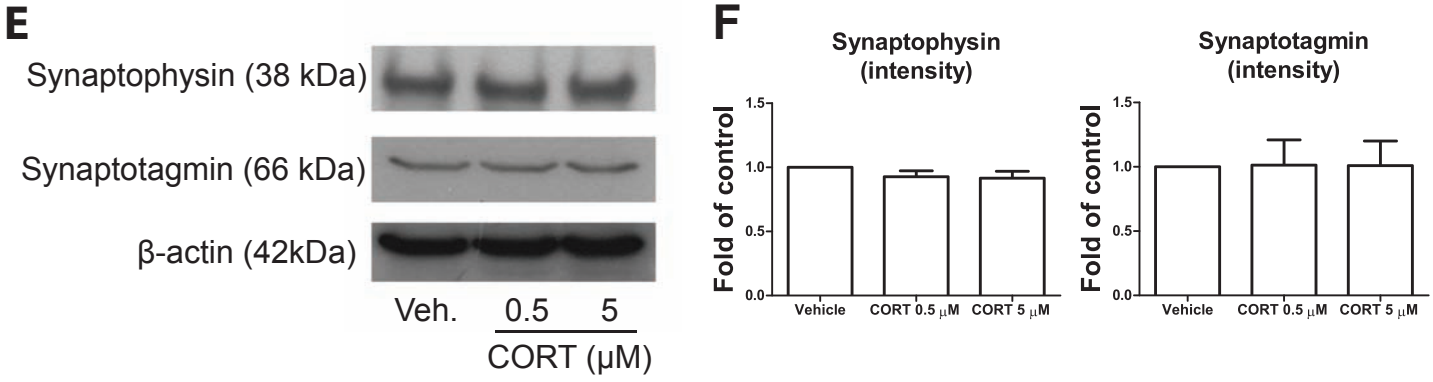

Fig. 2

Wuwongse et al., 2013

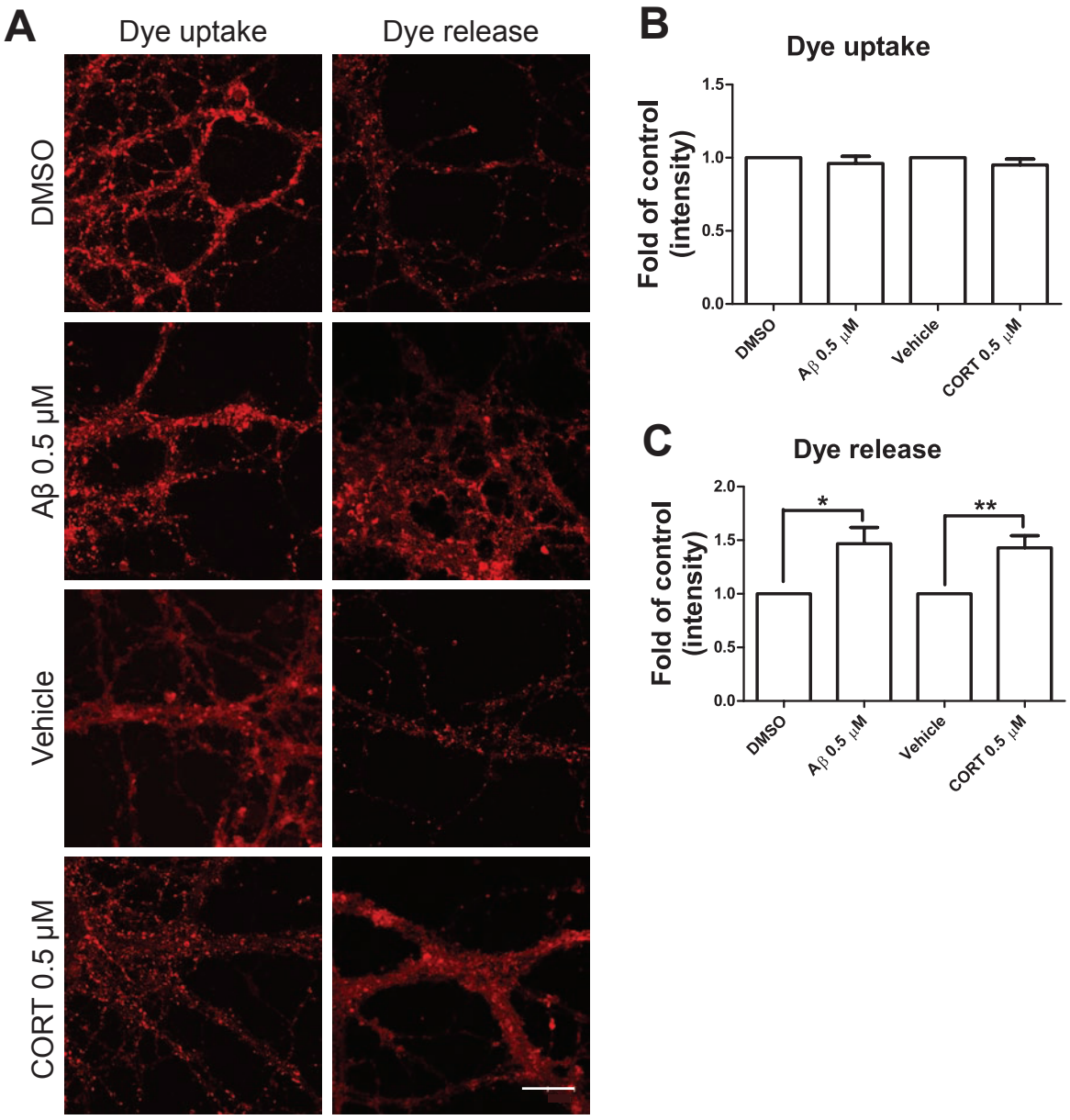

Fig. 3

Wuwongse et al., 2013

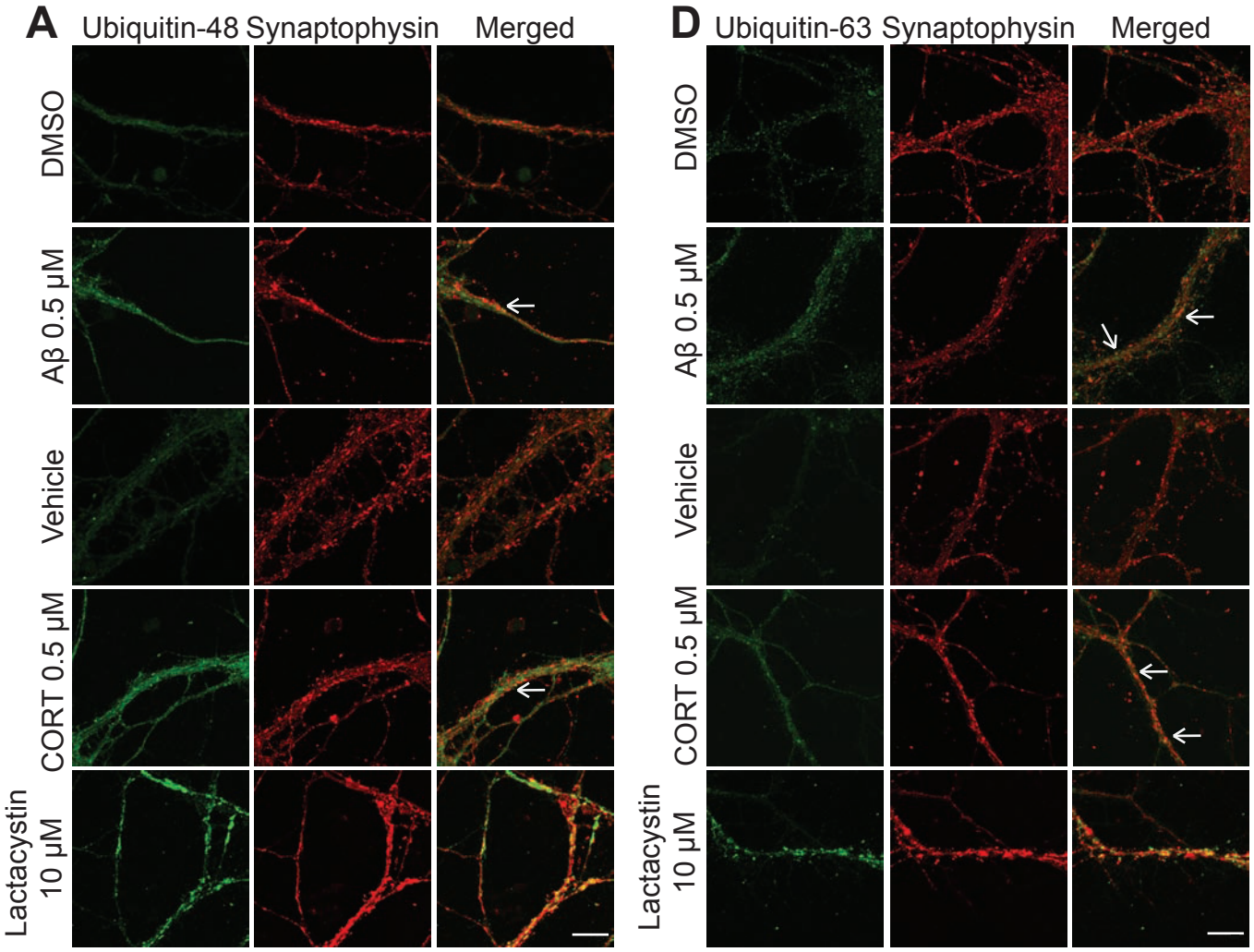

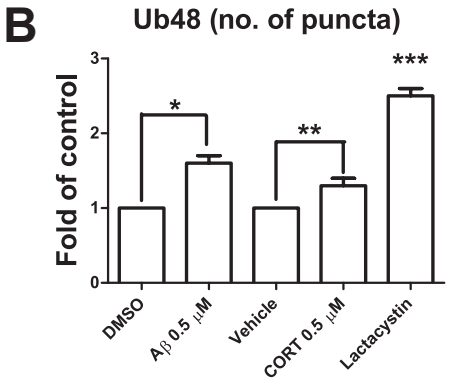

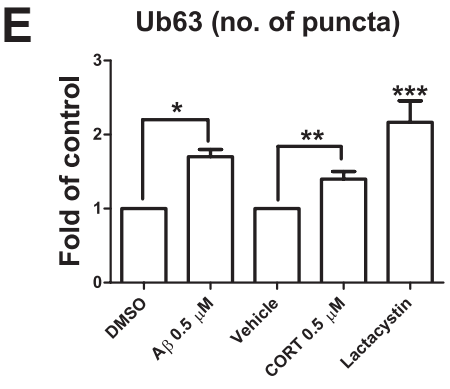

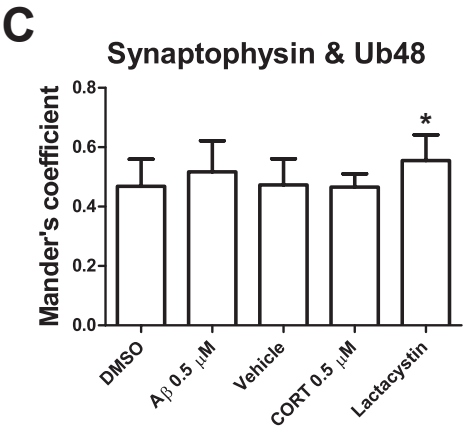

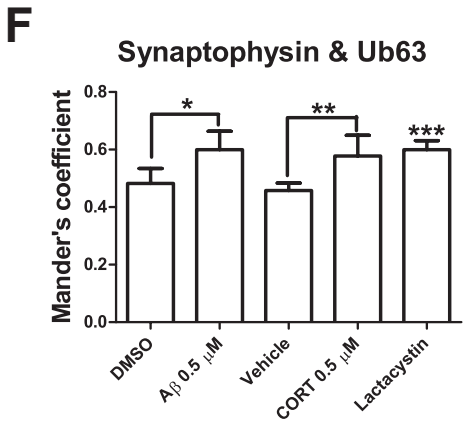

Fig. 4

Wuwongse et al., 2013

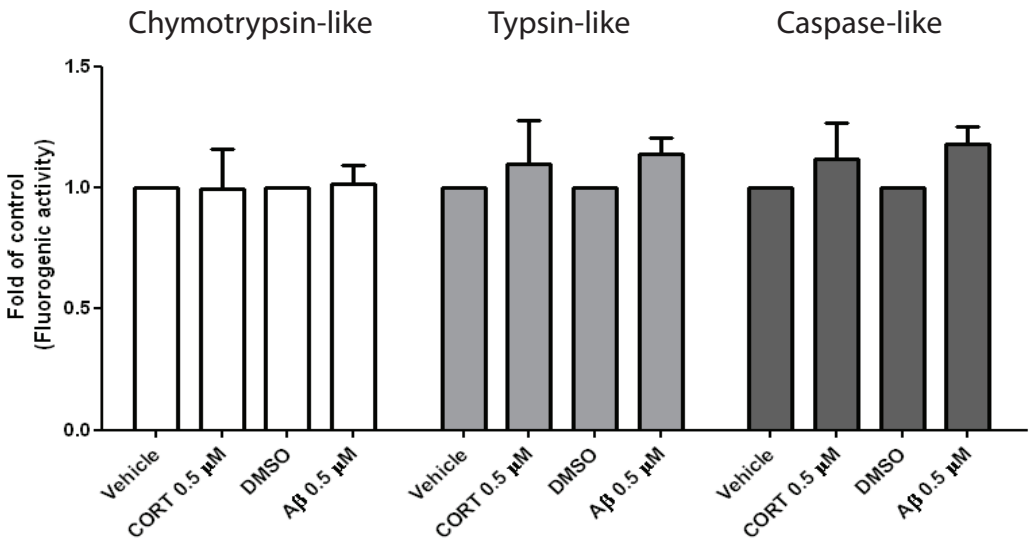

Fig. 5

Wuwongse et al., 2013

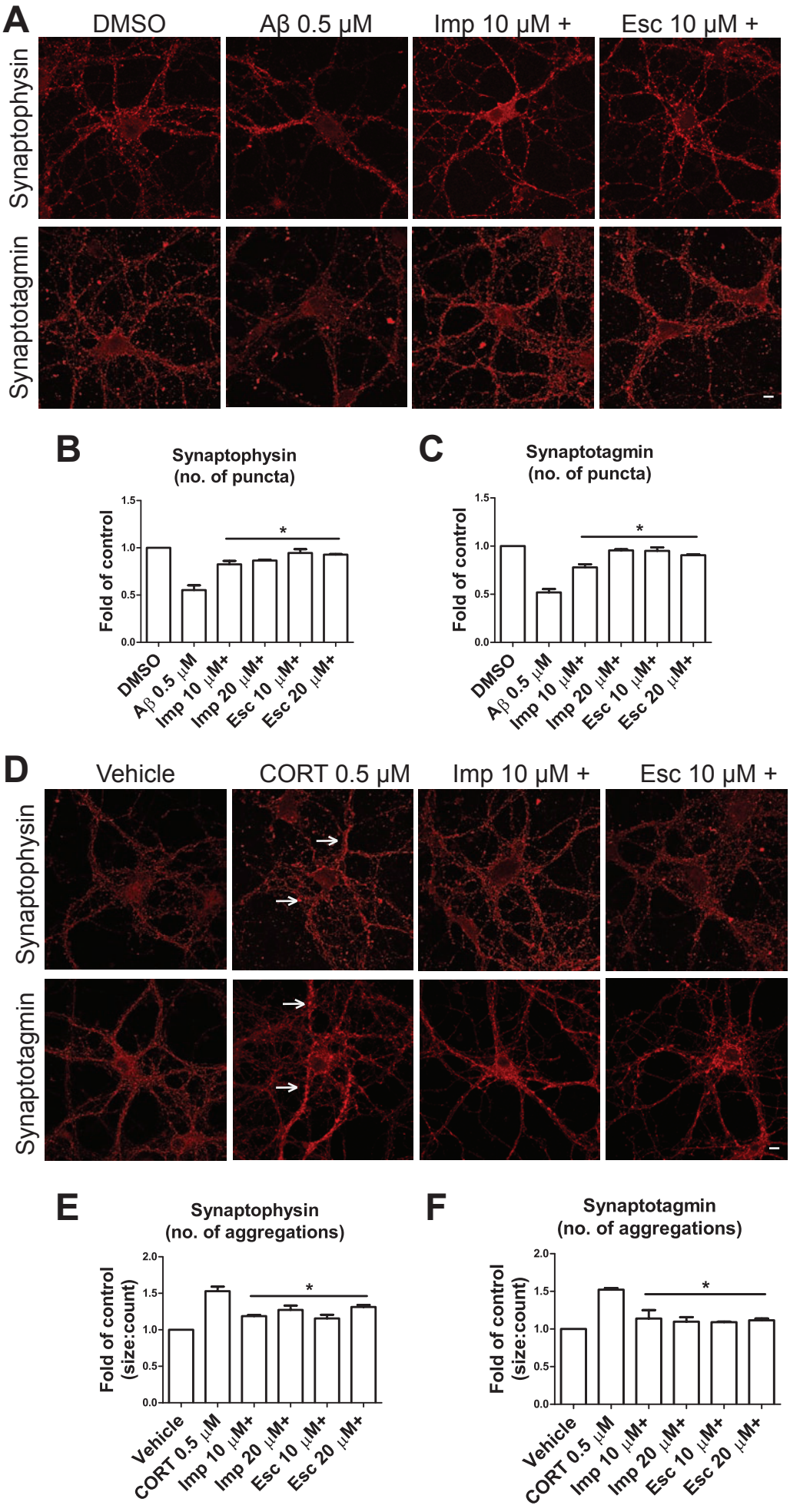

Fig. 6

Wuwongse et al., 2013

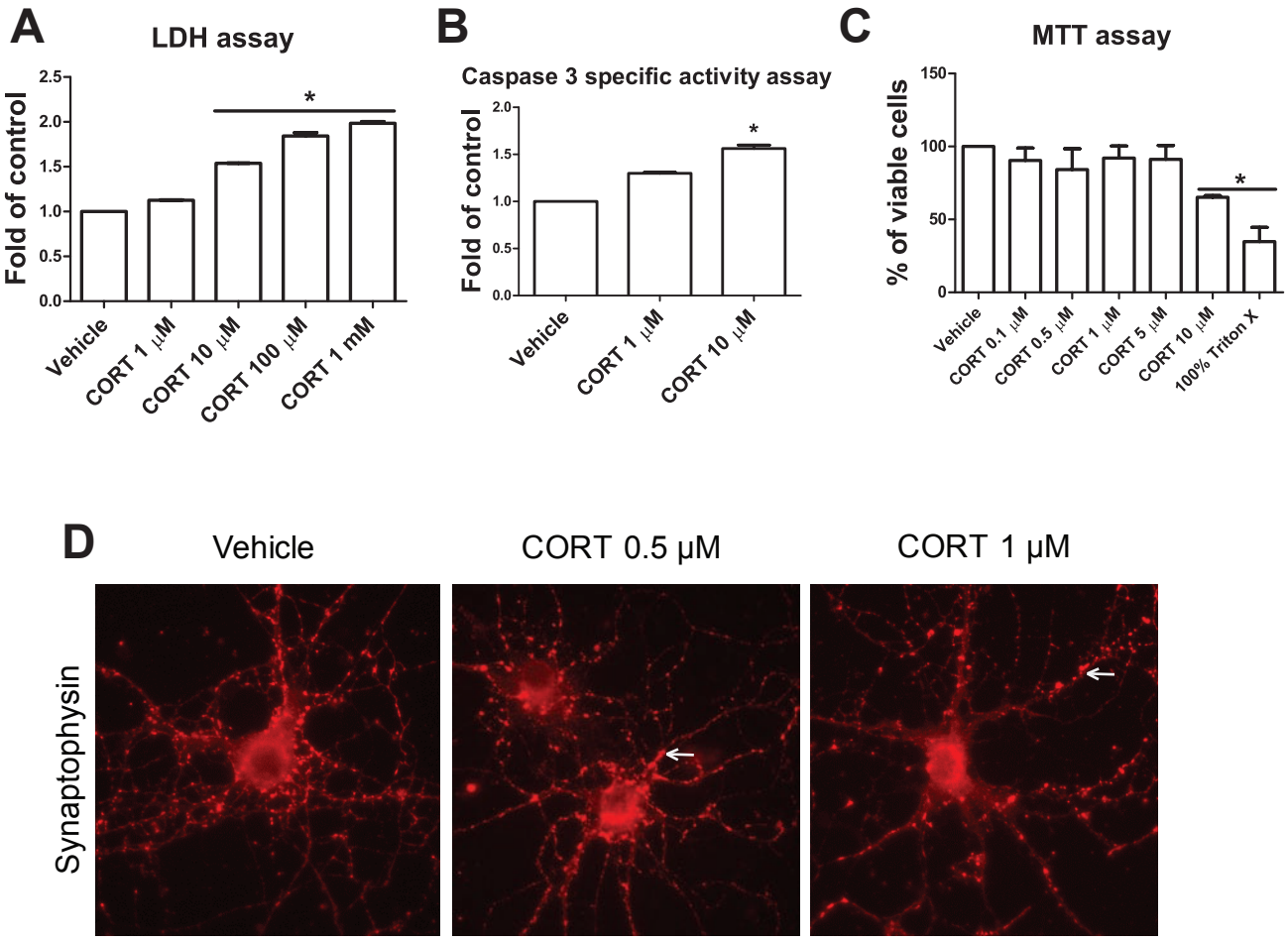
A
LDH assay
Fold of control
2.5
2.0
1.5
1.0
0.5
0.0
*
Vehicle
CORT 1 μM
CORT 10 μM
CORT 100 μM
CORT 1 mM
B
Caspase 3 specific activity assay
Fold of control
2.0
1.5
1.0
0.5
0.0
*
Vehicle
CORT 1 μM
CORT 10 μM
C
MTT assay
% of viable cells
150
100
50
0
*
Vehicle
CORT 0.1 μM
CORT 0.5 μM
CORT 1 μM
CORT 5 μM
CORT 10 μM
100% Triton X
D
Vehicle
CORT 0.5 μM
CORT 1 μM
Synaptophysin

A

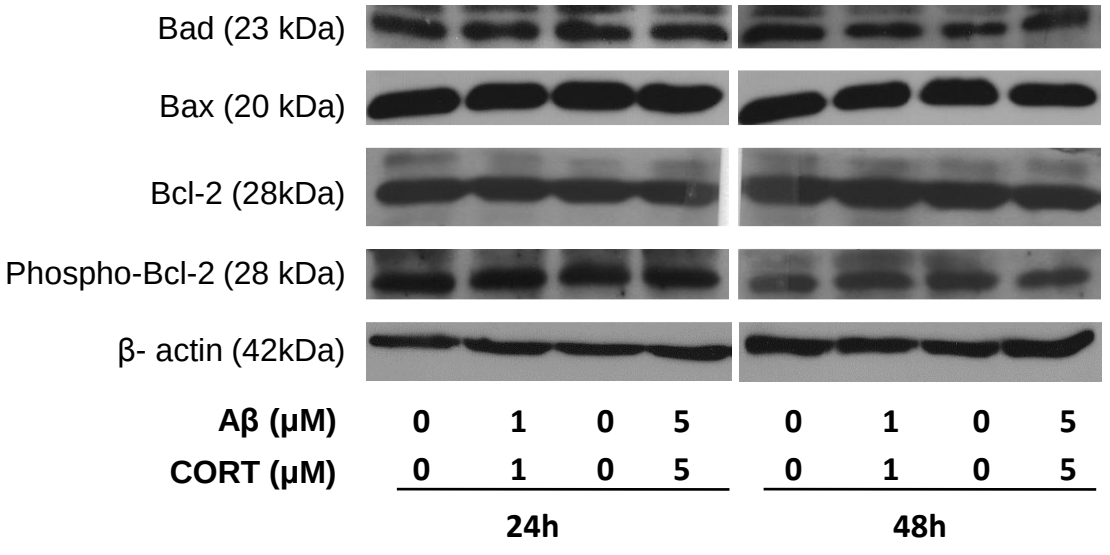

B

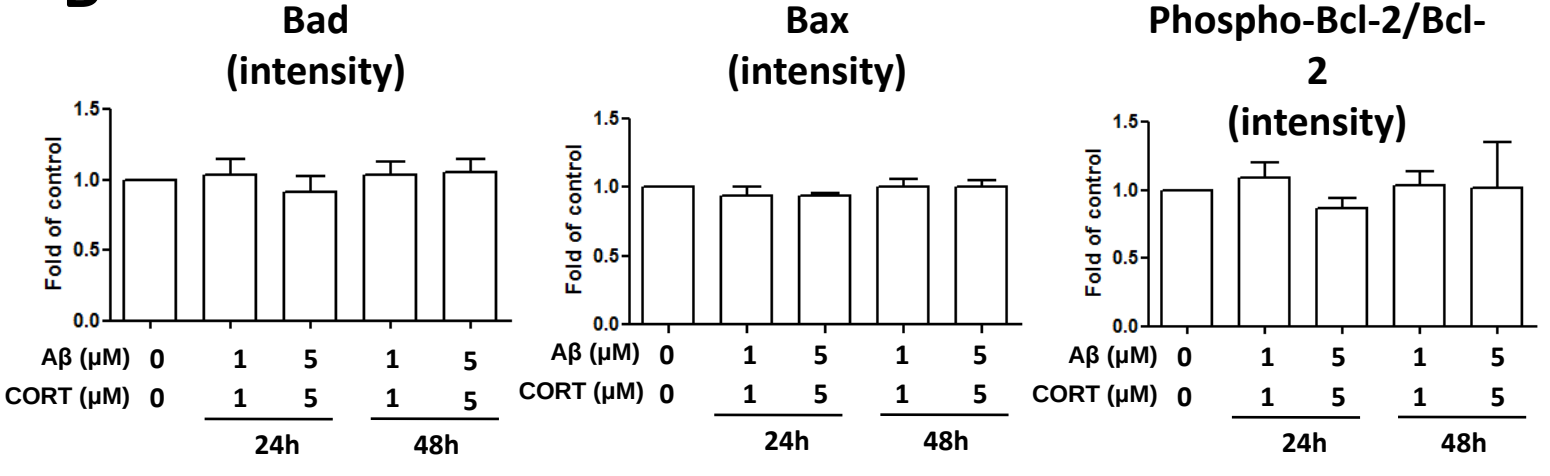

Supplementary Fig. 2

Wuwongse et al., 2013

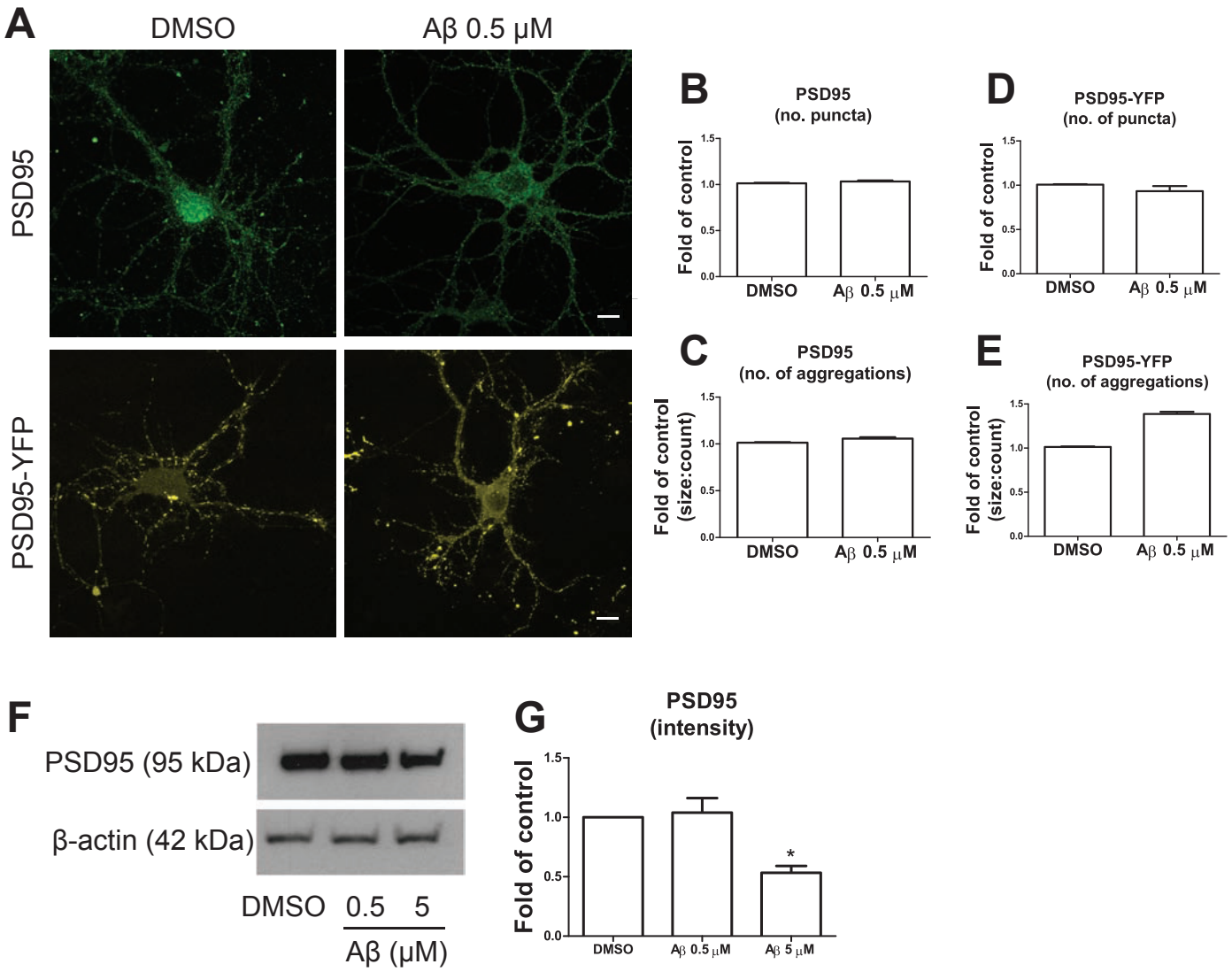
A
DMSO
Aβ 0.5 μM
PSD95
PSD95-YFP
B
PSD95
(no. puncta)
Fold of control
DMSO
Aβ 0.5 μM
D
PSD95-YFP
(no. of puncta)
C
PSD95
(no. of aggregations)
Fold of control
(size:count)
E
PSD95-YFP
(no. of aggregations)
F
PSD95 (95 kDa)
β-actin (42 kDa)
DMSO 0.5 5
Aβ (μM)
G
PSD95
(intensity)
Aβ 5 μM
*

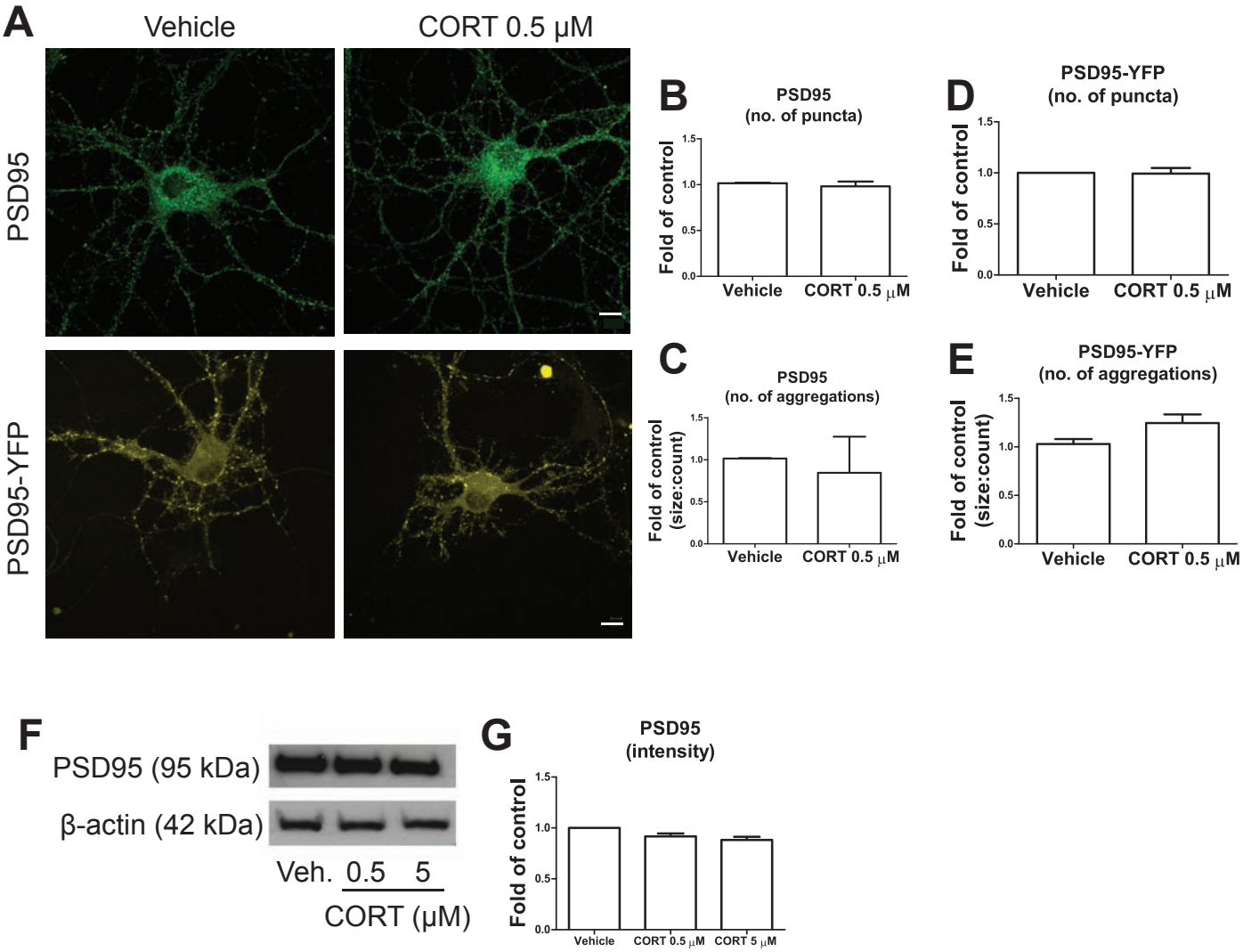
A
Vehicle
CORT 0.5 μM
PSD95
PSD95-YFP
B
PSD95
(no. of puncta)
Fold of control
Vehicle
CORT 0.5 μM
C
PSD95
(no. of aggregations)
Fold of control
(size:count)
Vehicle
CORT 0.5 μM
D
PSD95-YFP
(no. of puncta)
Fold of control
Vehicle
CORT 0.5 μM
E
PSD95-YFP
(no. of aggregations)
Fold of control
(size:count)
Vehicle
CORT 0.5 μM

F
PSD95 (95 kDa)
β-actin (42 kDa)
Veh. 0.5 5
CORT (μM)
G
PSD95
(intensity)
Fold of control
Vehicle
CORT 0.5 μM
CORT 5 μM

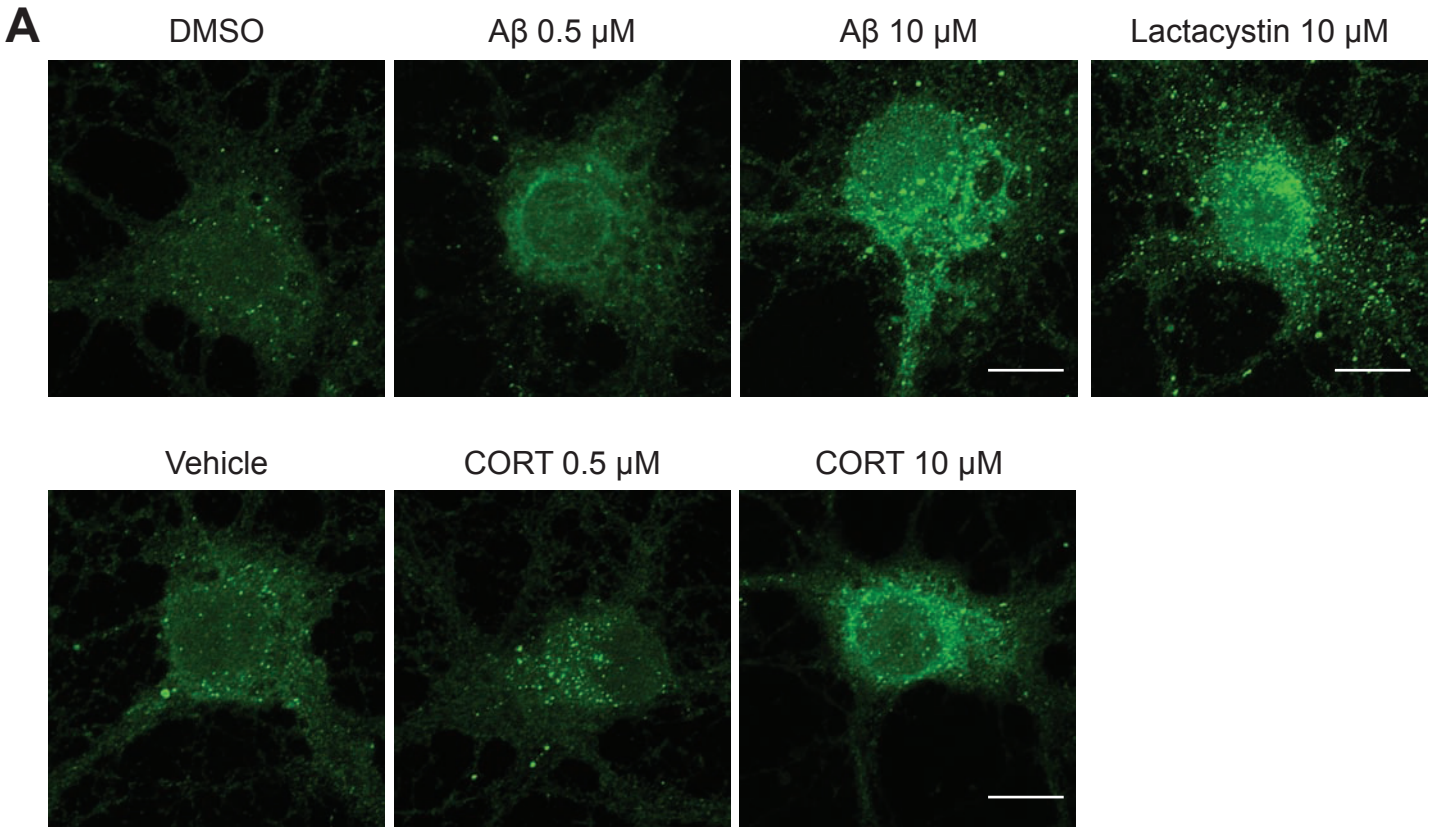
A
DMSO
Aβ 0.5 μM
Aβ 10 μM
Lactacystin 10 μM
Vehicle
CORT 0.5 μM
CORT 10 μM

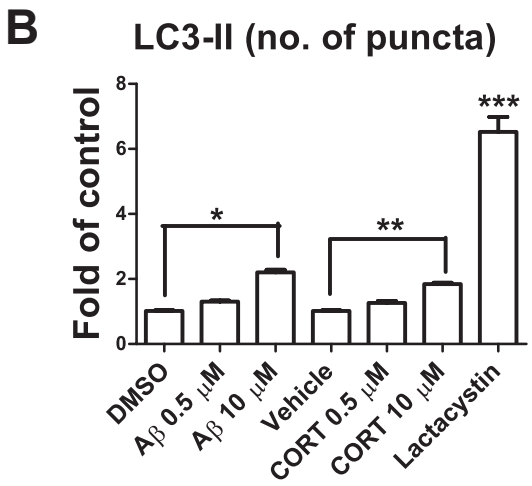
B
LC3-II (no. of puncta)
Fold of control
0
2
4
6
8
*
**
***
DMSO
Aβ 0.5 μM
Aβ 10 μM
Vehicle
CORT 0.5 μM
CORT 10 μM
Lactacystin

Supplementary Material (for online publication)
Click here to download Supplementary Material (for online publication): BBA Synaptic loss in MDD&AD Supplementary 070213a

Supplementary data

Materials and methods

Preparation of oligomeric Aβ1-42

Preparation of oligomeric Aβ1-42 was according to Lai et al., 2009 [1]. Synthetic human Aβ1-42 was purchased from the W.M. Keck Foundation Biotechnology Research Laboratory, Yale University (New Haven, USA). The peptide powder was dissolved in 1,1,1,3,3,3-hexafluoro-2-propanol (HFIP) (Sigma-Aldrich) to achieve the concentration of 2 mM of Aβ1-42 peptides. HFIP was then evaporated from the peptide solution. The remaining peptides were resuspended in anhydrous DMSO (Sigma-Aldrich), incubated in a bath sonicator for 30 min at room temperature, aliquoted and snap frozen in liquid nitrogen. The aliquoted peptide was then dissolved in culture medium to the desired concentration for treatment. Tris-Tricine gel electrophoresis was performed to examine the species of Aβ1-42 peptides within the preparation. The membrane was then incubated with mouse monoclonal anti-human Aβ (6E10) antibody (Signet, Hayward, CA, USA), followed by horseradish peroxidase-conjugated secondary antibody. Bands were visualized on Biomax X-ray film using ECL spray (Upstate, Syracuse, NY, USA).

Preparation of primary hippocampal cultures

Primary hippocampal neurons were prepared from embryonic day 18 Sprague-Dawley rats according to Lai et al., [1] (Laboratory Animal Unit, The University of Hong Kong, accredited by Association for Assessment and Accreditation of Laboratory Animal Care International. Approval for conducting experiments was obtained from the Committee on the use of Live Animals in Teaching and Research, The University of Hong Kong). Isolated hippocampi were dissociated in 1x PBS solution supplemented with 18 mM glucose and cultured on poly-L-lysine (25 μg/ml) coated 6-well plates (Iwaki, Japan), 12-well plates (Iwaki) with cover slips (Thermo Scientific), or MatTek culture dishes (MatTek, Ashland, MA, USA). Neurons were seeded at 6.5×10^5, 7.5×10^4 and 1.5×10^5 cells per well, respectively. Neurons were cultured in Neurobasal® medium (GIBCO-BRL, Rockville, MO, USA) supplemented with B-27, 2 mM L-glutamine, 10 μg/ml penicillin/streptomycin and 25 μM β-mercaptoethanol. Deoxyfluoridine was added to inhibit the growth of non-neuronal cells 1 day after seeding. Neurons were kept in a humidified incubator at 37°C and 5% CO_2 for 14 days prior to treatment.

Cell Culture of SH-SY5Y

Human neuroblastoma cell line SH-SY5Y cells were purchased from American Type Culture Collection (ATCC). Cells were cultured in supplemented MEM (2 mM L-glutamine, 50 units/ml penicillin, and 50 μg/ml streptomycin) with 10% heat-inactivated FBS and kept in a humidified incubator at 37˚C and 5% CO_2. Cells were seeded at 2 x

10^5 per well in 6-well plates for 2 days then treated with 1 or 5 μM of Aß and CORT for 24 and 48 hr.

Transfection

Neurons were cultured on MatTek glass-bottom dishes for transfection and live-cell imaging (Carl Zeiss, LSM510-Meta system). Transfection was done at DIV 7 for 4 hr with Lipofectamine 2000 (Invitrogen), treated on day 13 and analyzed 24 hr after treatment. Lipofectamine allows for high transfection efficiency and low neuronal toxicity [2]. PSD95-YFP was a gift from Prof. Rachel Wong (University of Washington, USA). Neurons were imaged using the LSM510 confocal microscope and images were quantified using MacBiophotonics Image J.

Cytotoxicity assay

Cytotoxicity was determined by the Cytotoxicity Detection kit (Roche, Mannheim, Germany) as described previously [3]. The assay measures LDH activity released from damaged cells. Briefly, culture medium was centrifuged and cell-free supernatant was collected and incubated in a 96-well plate with equal volumes of assay reagents (1 μl of reagent 1 to 44 μl of reagent 2) in the dark for 30 min. Absorbance was measured at 492 nm using the Multiskan Spectrum spectrophotometer. Results were expressed as fold of control.

Cell viability assay

Cell viability was measured by the [3-(4,5-dimethylthiazol-2-yl)-2,5-diphenyl tetrazolium bromide] (MTT) assay (Roche) as described previously [4]. In short, cells were incubated with MTT assay reagent 1 for 4 hr at 37˚C and 5% CO_2, followed by an overnight incubation period with reagent 2 at 37˚C and 5% CO_2. Absorbance was measured at wavelength 550 nm with reference wavelength at 690 nm by a microplate reader. Results were expressed as percentage of viable cells.

Caspase-3-like activity assay

After treatment with CORT and Aβ, cells were lysed using the caspase lysis buffer (1.192 g HEPES, 77.1 mg DTT, 2.95 mg EDTA, 0.002% Triton X-100, 100 ml milliQ H_2O) for caspase-3-like activity assay as described previously [5]. Total protein lysate was extracted to perform a protein assay to determine protein concentration, and 50 μg of protein was mixed with caspase-3 substrate (Ac-DEVD-pNA, 4 mM; Calbiochem), DTT (1 M) and 2X reaction buffer (50 μl), to a total volume of 100 μl. The mixture was duplicated for each sample and added into each well of a 96-well plate. The plate was then incubated at 37ºC for 2 hr and absorbance was measured at 405 nm using the Multiskan Spectrum spectrophotometer. Values of specific activity (pmol/min/μg) were calculated from the absorbance readings. Results were expressed as fold of control.

Antibodies

For western blot analysis, primary antibodies Bad (1:1000), Bax (1:1000), and phospho-Bcl-2 (1:1000) were incubated overnight at 4˚C (Cell Signaling). Bcl-2 (1:1000) (BD Biosciences) and PSD95 (1:2000) (Cell Signaling) were incubated for 4 hr at room temperature. β-actin (1:10000) was incubated for 1 hr at room temperature (Abcam).

For immunocytochemical analysis, PSD95 (1:400) (Synaptic System, Göttingen, Germany) was incubated for 1 hr at room temperature.

Analysis of fluorescent images

Quantitative measurements for intensity, puncta size and number of puncta were obtained by MacBiophotonics Image J. Protein aggregations were defined by size of puncta divided by number of puncta. Puncta quantification and co-localization analysis were performed using the Particle Analysis and Co-localization Analysis plug-in for MacBiophotonics Image J, respectively.

Results

Determination of CORT toxicity

LDH, MTT, and caspase-3-like activity assays were used to determine toxic concentrations of CORT to neurons. Ten micromolar of CORT for 24 hr induced neuronal cell death compared to control as seen by increased LDH release and caspase-3-like activity (Supplementary Fig. 1 A & B). MTT assay showed a significant decrease in percentage of viable cells after 24 hr treatment of 10 μM CORT (Supplementary Fig. 1 C). Treatment with 0.5 μM CORT was selected for subsequent experiments as observable changes to the pre-synaptic protein synaptophysin was observed without affecting cell viability (Supplementary Fig. 1 D).

Co-treatment with oligomeric Aβ and CORT did not induce changes in apoptotic marker expression

Since glucocorticoids have been found to increase neuronal vulnerability to treatments of various toxins [6], SH-SY5Y human neuroblastoma cells were co-treated with 1 or 5 μM of Aβ and CORT for 24 and 48 hr to examine whether CORT treatment would affect cell vulnerability in Aβ treated cells. Treatment of CORT did not induce changes to Bad or Bax expression or the ratio of phospho-Bcl-2 to Bcl-2 in cells also treated with Aβ (Supplementary Fig. 2), indicating that the presence of CORT does not affect neuronal survival in these cells.

Oligomeric Aβ and CORT caused post-synaptic damage

To investigate post-synaptic damage after Aβ and CORT treatment, primary hippocampal neurons were stained for PSD95 or transfected with PSD95-YFP. Both oligomeric Aβ and CORT treatment at 0.5 μM for 24 hr did not cause any statistically significant changes in number of puncta, number of aggregations or protein expression level of PSD95 (Supplementary Fig. 3 & 4).

Figure legends

Supplementary 1. Determination of CORT toxicity on primary culture of hippocampal neurons. A) Treatment of hippocampal neurons with CORT for 24 hr induced release of LDH significantly at 10 μM and above. Results were expressed as fold of control ± SE from at least 3 independent experiments. Statistical analysis was performed by one-way ANOVA, followed by the *post hoc* Tukey's test. * represents $p<0.05$ compared to the control. B) Treatment of primary hippocampal neurons for 24 hr with 10 μM CORT was able to significantly increase caspase-3-like activity, indicative of activation of downstream pathways involved in apoptosis. Results were expressed as fold of control ± SE from at least 3 independent experiments. Statistical analysis was performed by one-way ANOVA, followed by the *post hoc* Tukey's test. * represents $p<0.05$ compared to control. C) MTT assay results showed treatment of primary hippocampal neurons for 24 hr with CORT did not significantly affect the cell viability up to 10 μM. Treatment with 10% Triton X-100 served as a negative control. Results were expressed as percentage of

viable cells ± SE from at least 3 independent experiments. Statistical analysis was performed by one-way ANOVA, followed by the *post hoc* Tukey's test. * represents $p<0.01$ compared to control. D) Immunocytochemical analysis of synaptophysin showed that 0.5 and 1 μM CORT treatment caused observable protein aggregation (shown by arrows) using epifluorescent microscope (40x magnification), therefore 0.5 μM CORT was selected for subsequent experiments.

Supplementary 2. Low-dose CORT and oligomeric Aβ did not induce changes in apoptotic marker expression. A) Western blot analysis of SH-SY5Y cells treated with 1 and 5μM of CORT and Aβ for 24 and 48 hr did not show changes in the protein expression levels of Bad and Bax or ratio of phospho-Bcl-2 to Bcl-2. B) Quantitative analysis of western blot was performed by MacBiophotonics Image J. Results were expressed as fold of control ± SE from at least 3 independent experiments. Statistical analysis was performed by one-way ANOVA, followed by the *post hoc* Tukey's test.

Supplementary 3. Low-dose oligomeric Aβ treatment did not cause significant changes to the post-synaptic protein PSD95. A) Primary hippocampal neurons were transfected with PSD95-YFP on day 7 and imaged on day 14 or stained for PSD95 after treatment. Images were taken at using LSM510 confocal microscope at 63x objective (scale bar 10 μm). B-E) MacBiophotonics Image J was used to quantify the immunoreactivity by counting the number of positive puncta. Results were expressed as fold of control ± SE from at least 3 independent experiments. Statistical analysis was performed by unpaired *t*-test. F) Western blot analysis showed significantly reduced PSD95 protein levels after treatment with 5 μM Aβ. G) Quantitative analysis of western blot was performed by

MacBiophotonics Image J. Results were expressed as fold of control ± SE from at least 3 independent experiments. Statistical analysis was performed by one-way ANOVA, followed by the *post hoc* Tukey's test. * represents $p<0.05$ compared to corresponding control.

Supplementary 4. Low-dose CORT treatment did not cause significant changes to the expression of post-synaptic protein PSD95. A) Primary hippocampal neurons were transfected with PSD95-YFP on day 7 and imaged on day 14 or stained for PSD95 after treatment. Images were taken with LSM510 confocal microscope at 63x objective (scale bar 10 μm). B-E) MacBiophotonics Image J was used to quantify the immunoreactivity by counting the number of positive puncta. Results were expressed as fold of control ± SE from at least 3 independent experiments. Statistical analysis was performed by unpaired *t*-test. F) Western blot analysis showed no change in PSD95 protein level expression. G) Quantitative analysis of western blot was performed by MacBiophotonics Image J. Results were expressed as fold of control ± SE from at least 3 independent experiments. Statistical analysis was performed by one-way ANOVA, followed by the *post hoc* Tukey's test.

Supplementary 5. Oligomeric Aβ and CORT increased expression of autophagic marker, LC3-II. A) Primary hippocampal neurons were stained for immunoreactivity of LC3-II. Low-dose oligomeric Aβ and CORT (0.5 μM) did not significantly increase the number of LC3-II puncta compared to respective controls. However, treatment with 10 μM oligomeric Aβ and CORT for 24 hr significantly increased the number of LC3-II puncta.

Lactacystin served as a positive control. Images were taken with LSM510 confocal microscope at 63x objective (3x digital zoom; scale bar 10 μm). B) MacBiophotonics Image J quantitative analysis showed a significant increase in the number of LC3-II puncta with 10 μM of Aβ and CORT but not with 0.5 μM. Results were expressed as fold of control ± SE from at least 3 independent experiments. Statistical analysis was performed by one-way ANOVA, followed by the *post hoc* Tukey's test. *, **, & *** represents $p<0.05$, *0.01, and 0.001*, respectively, compared to the corresponding control.

References

[1] C.S. Lai, J. Preisler, L. Baum, D.H. Lee, H.K. Ng, J. Hugon, K.F. So, R.C. Chang, Low molecular weight Abeta induces collapse of endoplasmic reticulum, Mol Cell Neurosci, 41 (2009) 32-43.
[2] B. Dalby, S. Cates, A. Harris, E.C. Ohki, M.L. Tilkins, P.J. Price, V.C. Ciccarone, Advanced transfection with Lipofectamine 2000 reagent: primary neurons, siRNA, and high-throughput applications, Methods, 33 (2004) 95-103.
[3] Y.S. Ho, X. Yang, J.C. Lau, C.H. Hung, S. Wuwongse, Q. Zhang, J. Wang, L. Baum, K.F. So, R.C. Chang, Endoplasmic reticulum stress induces tau pathology and forms a vicious cycle: implication in Alzheimer's disease pathogenesis, J Alzheimers Dis, 28 (2012) 839-854.
[4] Y.T. Cheung, W.K. Lau, M.S. Yu, C.S. Lai, S.C. Yeung, K.F. So, R.C. Chang, Effects of all-trans-retinoic acid on human SH-SY5Y neuroblastoma as in vitro model in neurotoxicity research, Neurotoxicology, 30 (2009) 127-135.
[5] Y.T. Cheung, N.Q. Zhang, C.H. Hung, C.S. Lai, M.S. Yu, K.F. So, R.C. Chang, Temporal relationship of autophagy and apoptosis in neurons challenged by low molecular weight beta-amyloid peptide, J Cell Mol Med, 15 (2011) 244-257.
[6] I. Abrahám, T. Harkany, K.M. Horvath, A.H. Veenema, B. Penke, C. Nyakas, P.G. Luiten, Chronic corticosterone administration dose-dependently modulates Abeta(1-42)-and NMDA-induced neurodegeneration in rat magnocellular nucleus basalis, J Neuroendocrinol, 12 (2000) 486-494.